

Australia going down under: Quantifying continental subduction during arc-continent accretion in Timor-Leste

Garrett W. Tate¹, Nadine McQuarrie², Douwe J.J. van Hinsbergen³, Richard R. Bakker⁴, Ron Harris⁵, and Haishui Jiang⁶

¹Chevron Corporation, 1500 Louisiana Street, Houston, Texas 77002, USA

²Department of Geology and Planetary Science, University of Pittsburgh, 4107 O'Hara St, SRCC Room 200, Pittsburgh, Pennsylvania 15260, USA

³Department of Earth Sciences, Utrecht University, Budapestlaan 4, 3584 CD Utrecht, Netherlands

⁴Department of Earth Sciences, ETH Zurich, NO D 51.3, Sonneggstrasse 5, 8092 Zurich, Switzerland

⁵Department of Geological Sciences, Brigham Young University, S389 ESC, Provo, Utah, 84602, USA

⁶Earth Sciences, China University of Geosciences, 388 Lumo Road, Wuhan, Hubei Province, 430074 China

ABSTRACT

Models of arc-continent accretion often assume that the period of subduction of continental lithosphere before plate boundary reorganization is fairly short lived, yet the timescale of this period is poorly constrained by observations in the geologic record. The island of Timor is the uplifted accretionary complex resulting from the active collision of the Banda volcanic arc with the Australian continental margin. The exposure of underplated and exhumed Australian strata on Timor allows for the characterization of the structural history of accretion of uppermost Australian crust and the quantification of subduction of its original continental lithospheric underpinnings. New structural mapping in East Timor (Timor-Leste) reveals that duplexing of a 2-km-thick package of Australian continental strata has built the majority of the structural elevation of the Timor orogen. Coupling new structural observations with previous thermochronology results reveals the sequence of deformation within the orogen, the presence of subsurface duplexing below the hinterland slate belt, and motion along a foreland subsurface thrust ramp. Construction of balanced cross sections allows for the quantification of the amount of shortening in the orogen, and from that, the length of the subducted Australian continental lithosphere. Two balanced cross sections in East Timor reveal 326–362 km of shortening and that 215–229 km of Australian continental lithosphere have been subducted below the Banda forearc. These results highlight the fact that considerable amounts of continental lithosphere can be subducted while accreting only a thin section of uppermost crust. Continental subduction may have been favorable at Timor because of fast subduction rates, old oceanic crust at the consumed Australian margin, and subduction of some length of transitional crust. These results provide quantitative constraints for future numerical modeling of the geodynamics of continental subduction and arc-continent collision.

INTRODUCTION

The canonical view in plate tectonics has long been that oceanic lithosphere subducts and that continental lithosphere cannot (McKenzie, 1969). However, geological and geophysical studies of orogenic belts that

formed at subduction zones have shown, for example, that microcontinental blocks may subduct partly without leading to slab breakoff (van Hinsbergen et al., 2005; Capitanio et al., 2010). Also, passive margins of major continents may partly subduct upon arrival in a subduction zone during continent-continent collision, for example, in Arabia (Agard et al., 2011; Mouthereau et al., 2012; McQuarrie and van Hinsbergen, 2013) and India (Long et al., 2011). Quantifying the rate and amount of continental subduction is a key factor toward unraveling the dynamics of continental subduction and to the understanding of the terminal phases of a subduction zone.

Arc-continent collision is a key step in the tectonic cycle, marking the arrival of continental lithosphere at a volcanic arc that formed above an intra-oceanic subduction zone (Wilson, 1966; Dewey and Bird, 1970). This process is ubiquitous in the geologic record and has played a key role in forming the continental masses that are seen today (Şengör et al., 1993). Arc-continent accretion has been accommodated by a number of different deformation styles and tectonic plate geometries (e.g., Dickinson and Lawton, 2001). However, this paper will focus on the following canonical sequence of deformation from Dewey and Bird (1970): (1) Oceanic lithosphere is consumed in a subduction zone below an intra-oceanic volcanic arc. (2) A continental passive margin located updip of the subducting oceanic slab is brought into contact with the island arc and forearc through continued subduction. (3) Thrust slices of the island arc are emplaced on deformed rocks of the continental margin. (4) Continental subduction ceases and convergence becomes accommodated elsewhere, such as in a new subduction zone on the opposite side of the island arc. After this process, a piece of overriding oceanic plate (an ophiolite) and associated rocks are located structurally above the continental crust.

When continental crust is brought into a subduction zone as a part of the downgoing plate, the combined effects of lower density and greater thickness of continental crust produce buoyant forces that eventually inhibit continental subduction (McKenzie, 1969). McKenzie (1969) proposed that it is this attempted subduction of continental material that ends the process of arc accretion and causes reorganization of the plate boundaries through a switch in subduction polarity, changes in overall plate motions, or both.

It is unclear, however, exactly how much continental crust can be subducted before plate boundary reorganization or plate motion changes are observed. Early models of arc-continent accretion assumed subduction migration behind the island arc was a nearly instantaneous response to continental subduction (McKenzie, 1969; Dewey and Bird, 1970). However, the presence of coesite and diamond within gneisses of ultrahigh-pressure (UHP) terranes requires a mechanism for subduction of continental material to pressures of 2.7–4 GPa and to depths greater than 100–120 km prior to exhumation (Chopin, 1984; Smith, 1984; Sobolev and Shatsky, 1990; Hermann and Rubatto, 2014). In the Mediterranean, subduction of microcontinental blocks proceeded for hundreds of kilometers, accreting upper crust and subducting continental lower crust and mantle lithosphere without slab breakoff (van Hinsbergen et al., 2005; van Hinsbergen et al., 2010). Cloos (1993) calculated that granitic continental crust 25 km thick is able to be subducted if it is mechanically linked to a lithospheric mantle that extends to a depth of 200 km, although an effective mechanical link was questioned. Other models have shown that subduction of continental lower crust and mantle lithosphere can be favorable if upper crust is removed and accreted to the overriding plate (Capitanio et al., 2010). Numerical models of slab breakoff during continental collision have suggested subduction of continental crust to depths of ~120 km before slab breakoff (Baumann et al., 2010), with some suggesting possibly greater depths of continental subduction for subduction rates faster than 1 cm/yr (Davies and von Blanckenburg, 1995). More recent numerical models of slab breakoff during continental collision indicate that slab breakoff is expected at the continent-ocean transition at depths positively correlated to the age of the oceanic crust, with breakoff at depths of 300 km for 80 Ma oceanic crust and both upper and lower continental crust subducted to depths of 200 km or greater (Duretz et al., 2011; van Hunen and Allen, 2011).

The island of Timor is a modern example of arc-continent collision between the Banda arc and the Australian margin (Carter et al., 1976). Timor represents the earliest stages of arc accretion compared to other modern analogues such as Taiwan and New Guinea, because only the Banda forearc is found thrust upon Timor today and the volcanic arc remains separated from Timor by a shortened forearc basin (Huang et al., 2000). Nevertheless, global positioning system (GPS) measurements indicate that much of the convergence between Australia and Sunda at the longitude of Timor is accommodated north of the Banda arc, suggesting that plate boundary reorganization may now be beginning (Nugroho et al., 2009). Timor, therefore, is a prime locale for evaluating the magnitude and rates of continental subduction during arc accretion.

Here we present new structural mapping of central East Timor (Timor-Leste) and two corresponding balanced cross sections through the orogen. These balanced cross sections constrain minimum shortening amounts during arc-continent collision. Furthermore, restored lengths of stratigraphy from the downgoing plate that was underplated to the island during orogenesis allow us to constrain the length of subducted continental lithosphere.

■ GEOLOGIC SETTING

Timor is located at the collisional margin between the oceanic Banda volcanic arc and the Australian continental margin (Fig. 1). Early mapping documented structural deformation of Australian-affinity strata below allochthonous material with affinity to the Banda arc (Audley-Charles, 1968). Using the early mapping of Audley-Charles (1968) as a base, subsequent interpretations of mapped relationships suggest duplexing of Permian–Jurassic Australian sedimentary strata below an overthrust oceanic Banda forearc klippe, with Cretaceous and younger Australian strata deformed at the front of the Banda klippe (Carter et al., 1976; Harris, 1991, 2006; Zobell, 2007). However, the locations of duplex faults and the stratigraphy involved in duplexing have not been documented in detail. This is a key element of our study, since it is essential information to determine the amount of shortening and continental subduction.

To place the amount of continental subduction in its plate kinematic context, it is imperative to know the age of collision, which is debated. Stratigraphic constraints require orogenesis at Timor after 9.8 Ma, the ages of youngest Australian passive margin strata within the thrust belt on Timor-Leste (Keep and Haig, 2010), and before 5.6–5.2 Ma, the oldest synorogenic sediments deposited on a tectonic mélange that formed during orogenesis (Harris et al., 1998; Haig and McCartney, 2007). $^{40}\text{Ar}/^{39}\text{Ar}$ thermochronology suggests earliest exhumation of underplated Australian continental material at 7.13 ± 0.25 Ma (Tate et al., 2014) or ca. 7.5–8 Ma (Berry and McDougall, 1986). Some debate remains over whether these cooling ages reflect processes within the Banda forearc or initial collision between the Banda forearc and the distal-most Australian margin. Detrital zircon ages of ca. 290 Ma have been used to argue that these units with $^{40}\text{Ar}/^{39}\text{Ar}$ ages >7 Ma belong to fragments of the Sula Spur (a continental ribbon that rifted off Australia in the Mesozoic) that were incorporated within the Banda forearc before Banda-Australia collision (Ely et al., 2014). However, because similar detrital zircon peaks of 254–358 Ma have been found within other Australian-affinity units of the Gondwana Sequence (Zobell, 2007), a derivation from the Sula Spur is not required. The continuation of volcanism at Wetar until 3 Ma (Abbott and Chamalaun, 1981) or even 2.4 Ma (Herrington et al., 2011) and at Atauro until 3.3 Ma (Ely et al., 2011) has been used as an argument against initial collision of the distal Australian margin with the Banda arc before 4 Ma (Audley-Charles, 2011). However, He, Pb, and Sr isotopic signals from Banda arc volcanics demonstrate contamination of the magma source with continental material, supporting subduction of continental material to depths of magma generation from 5 to 2.4 Ma (Elburg et al., 2004; Herrington et al., 2011) and therefore initial collision of the Banda forearc and Australian margin even earlier.

Thermochronologic and sedimentologic observations also constrain the age of emergence and the rate of continued deformation on Timor. The emergence of Timor-Leste above water is suggested to be shortly before 4.45 Ma by Nguyen et al. (2013) as indicated by increased clastic input and

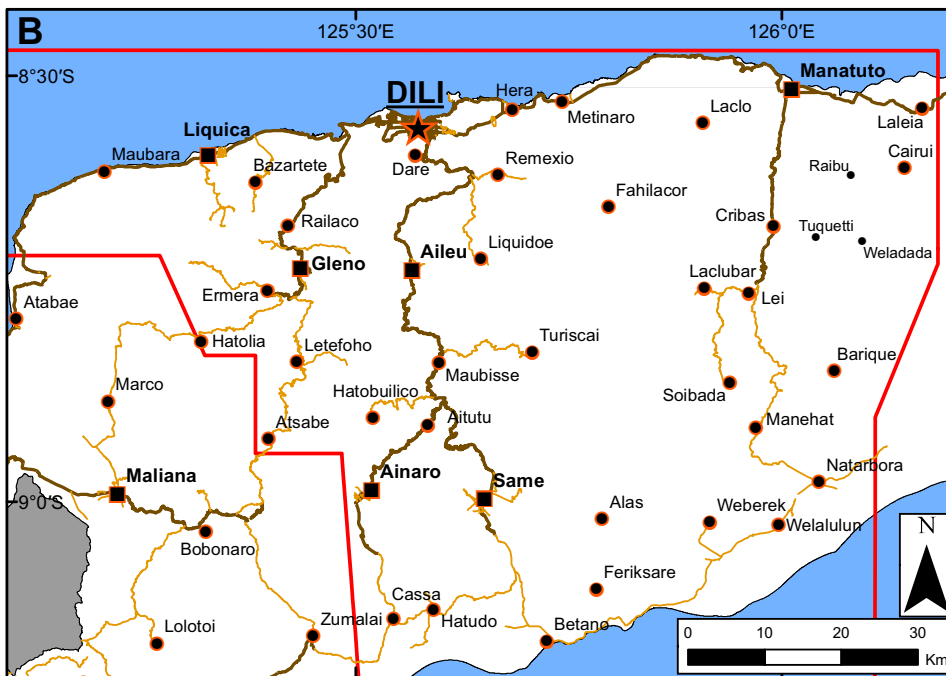
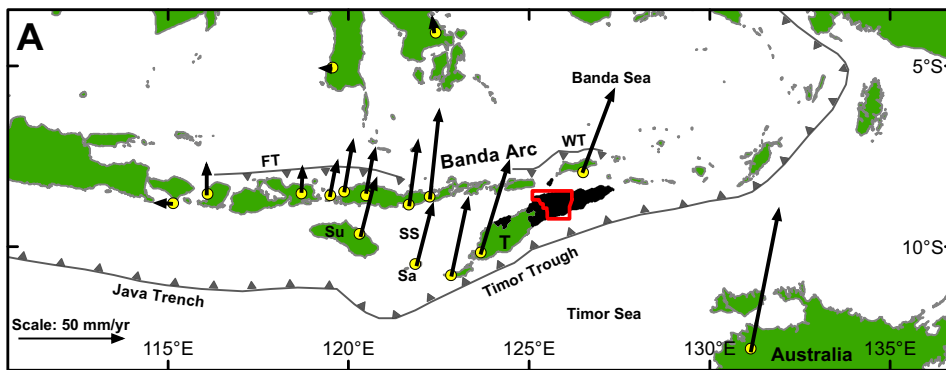


Figure 1. (A) Regional setting, with Timor-Leste in black and study area outlined in red. Global positioning system (GPS) vectors relative to fixed Asia from Nugroho et al. (2009). T—Timor; Su—Sumba; Sa—Savu; SS—Savu Sea; FT—Flores thrust; WT—Wetar Thrust. (B) Location reference of study area, with major towns referenced in text.

increased mangrove and lowland rainforest pollen in synorogenic deposits. Tate et al. (2014) use low-temperature thermochronology to document an extremely heterogeneous history of exhumation across the map area of this paper, with apatite and zircon (U-Th)/He ages ranging from 1.5 to 5.5 Ma with larger exhumation magnitudes and faster exhumation rates in the hinterland slate belt compared to the more foreland fold-thrust belt in the south and east. Continued rapid uplift on Timor and the Banda arc is also evident, with Quaternary coral terraces uplifted up to 700 m on Atauro (Ely et al., 2011) and with similar coral terraces present on the north coast of Timor-Leste (Audley-Charles, 1968; Cox, 2009). Significant debate remains as to the active mode of deformation on Timor today, with various interpretations spanning active duplexing of Australian strata (Tate et al., 2014), arc-parallel extrusion along transtensional faults (Duffy et al., 2013), and extension driven by slab breakoff and isostatic rebound (Keep and Haig, 2010).

Plate reconstructions and GPS measurements both indicate that Australia is moving north relative to the Sunda arc and South Banda arc at ~7 cm/yr (Nugroho et al., 2009; Spakman and Hall, 2010; Seton et al., 2012). Modern convergence is oblique, with ~53 mm/yr of convergence perpendicular to the Timor Trough (the deformation front of the Timor orogen) (Nugroho et al., 2009). Along the trend of Timor this convergence is partitioned between the Timor Trough and the Wetar Thrust, with ~20 mm/yr of convergence partitioned between Australia and Timor and ~33 mm/yr of convergence accommodated between Wetar and the Sunda block (Nugroho et al., 2009). It appears, therefore, that plate boundary reorganization may be under way at Timor. Another argument to that end comes from seismological observations that a seismic gap exists in the downgoing slab below Wetar that may indicate ongoing or recent slab breakoff (McCaffrey et al., 1985; Sandiford, 2008; Ely and Sandiford, 2010). We note, however, that such a seismic gap does not uniquely indicate slab breakoff, since a similar seismic gap below Taiwan is attributed to the subduction of continental material that would lack the water content necessary for typical slab dehydration earthquakes (Chen et al., 2004). In addition, seismic tomography does not image a gap in the slab below Wetar (Spakman and Hall, 2010).

TECTONOSTRATIGRAPHY

Australian-Affinity Units

Australian-affinity units are those deposited on Australian continental or transitional continental crust prior to collision with the Banda Terrane. The units deposited within intracratonic basins prior to the breakup of Gondwana are collectively referred to as the Gondwana Sequence (Harris et al., 1998). The Gondwana Sequence consists primarily of the Cribas, Maubisse, Aitutu, and Wailuli formations and also includes the Atahoc, Niof, and Babulu formations (Fig. 2).

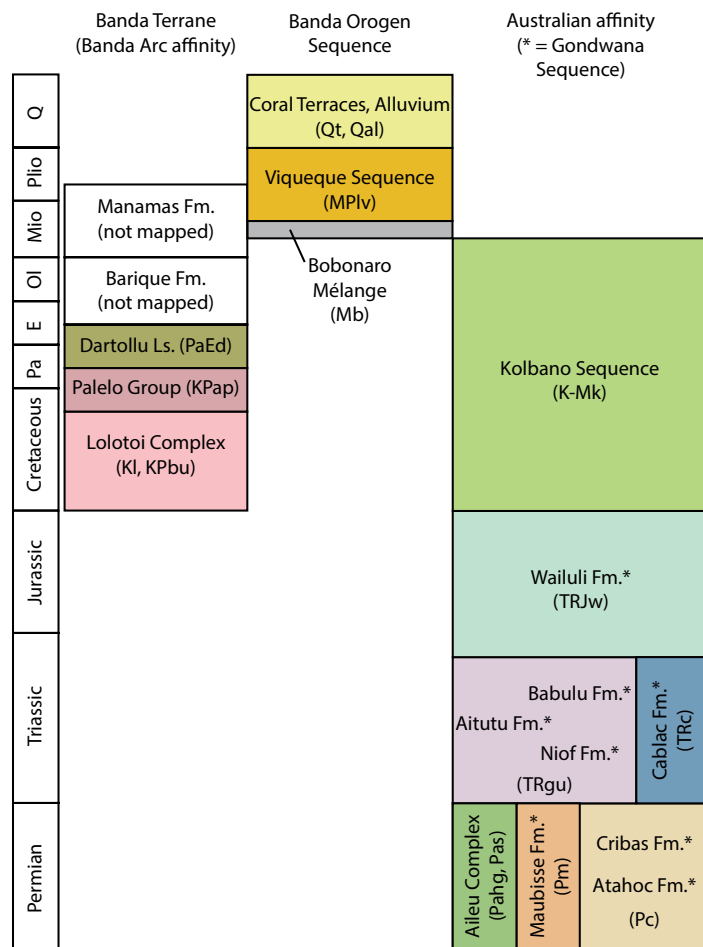


Figure 2. Tectonostratigraphy of Timor-Leste. Units belonging to the Gondwana Sequence are indicated by an asterisk. The Bobonaro mélangé formed during orogenesis in the late Miocene, but its matrix is sourced from the Wailuli Formation, and it is most commonly found in a tectonostratigraphic position above the Gondwana Sequence duplex. Units are colored consistently with the map and cross sections. Map unit labels are included in parentheses.

Permian Cribas and Atahoc Formations

Audley-Charles (1968) defined the Cribas and Atahoc formations as a Lower to Upper Permian succession of Australian-affinity units. Both formations have been interpreted as deposits within Australian intracratonic rift basins (Bird and Cook, 1991). We find the Cribas Formation to contain black shales and brown siltstones, with medium- to thick-bedded coarse calcarenites and occa-

sional limestones (Figs. 2 and 3A). Ironstone and claystone nodules are common in the shales. Some fossiliferous calcarenites and limestones are also present, containing plentiful crinoids and ammonites. Rare volcanic breccias (near Tuquetti; towns referenced found in Fig. 4) and basalt layers are also observed within the Cribas Formation. The Atahoc Formation presents very similar lithologies, with black shales and silty shales containing common ironstone and claystone nodules and occasional siltstones and sandstones. The amygdaloidal basalt used by Audley-Charles (1968) as the stratigraphic contact between the Upper Permian Cribas and Lower Permian Atahoc formations is rarely exposed outside of the type location. It is likely this basalt covered limited map extent in its original depositional environment in the Permian compared to the widespread occurrence of the clastic units. We therefore use the convention of referring to the Atahoc and Cribas together simply as the Cribas Formation, with a mapped thickness of 1 km.

Maubisse Formation

The Maubisse Formation was described by Audley-Charles (1968) as a 900-m-thick unit of massive fossiliferous limestones weathering dark red, as well as thick successions of mafic extrusive rocks. The Maubisse Formation is mainly Permian in age (Charlton et al., 2002), with a few sections dated as Latest Carboniferous (Davydov et al., 2013, 2014). We find the Maubisse Formation to consist of massive gray limestone weathering dark red, containing plentiful ammonites, crinoids, and other fossils and interbedded with thick basalts and mafic volcanoclastics (Fig. 3B). Portions of the Maubisse Formation contain shale and silty shale usually weathering brown to red. Although originally identified as an allochthonous unit (Audley-Charles, 1965), Charlton et al. (2002) conclude that the Maubisse Formation was deposited on shallow horst blocks of Australia roughly contemporaneously with deposition of the Atahoc and Cribas formations in the deeper grabens. This lateral relationship in the original depositional environment is further supported by our observation of occasional 20-cm-thick red-weathering fossiliferous limestones within the lower Cribas Formation near Tuquetti interbedded with shale containing ironstone nodules.

Aileu Complex

The Aileu Complex has been previously described as a wide metamorphic belt with slates, phyllites, metavolcanics, quartzites, marbles, and amphibolites (Audley-Charles, 1968; Berry and Grady, 1981; Charlton et al., 2002). A Permian age is attributed to the sedimentary protoliths of the unit based on lightly metamorphosed fossil beds (Audley-Charles, 1968). Although originally identified as allochthonous (Audley-Charles, 1968), Prasetyadi and Harris (1996) propose the para-autochthonous Cribas and Maubisse formations as protoliths of the Aileu based on similarities in lithology and fossil content. As

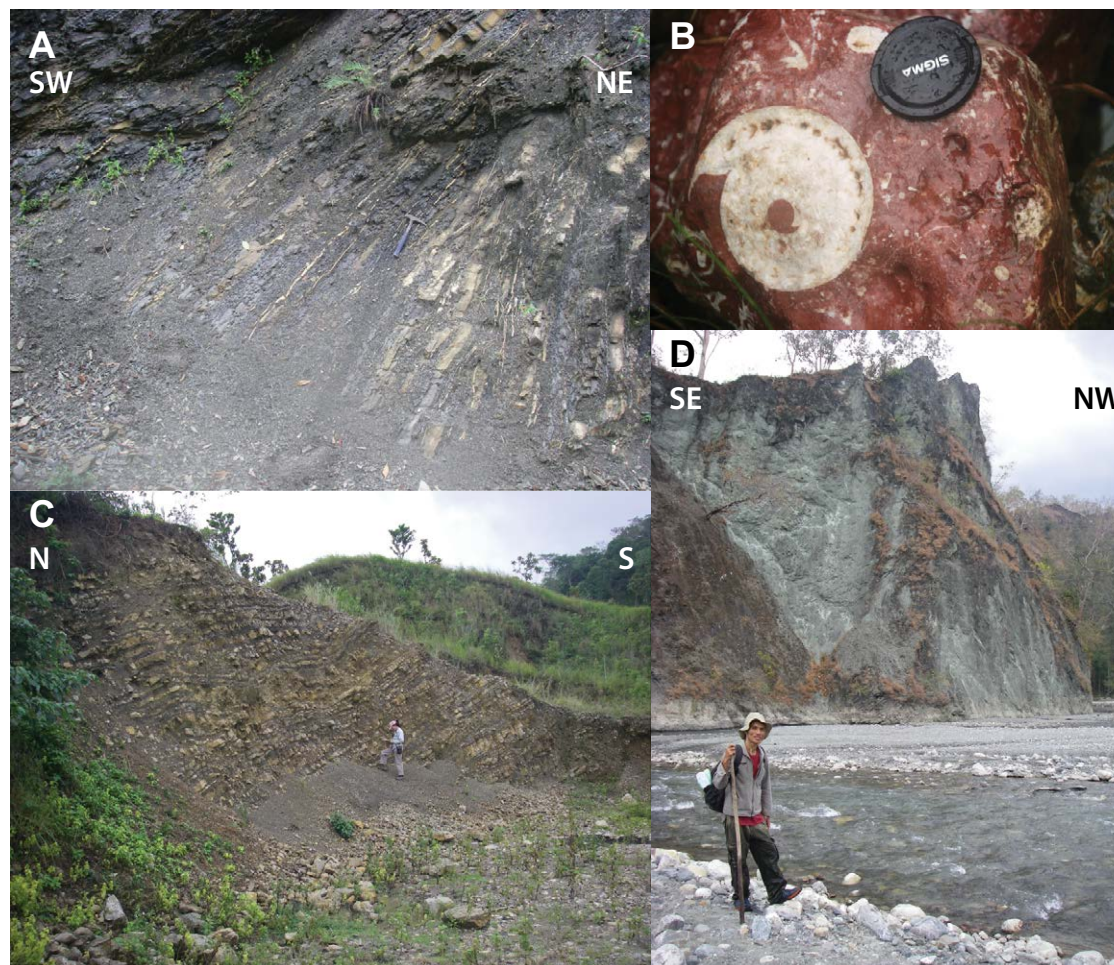


Figure 3. Field photographs of select stratigraphic units. (A) Cribas Formation between Aituto and Same. (B) Boulder of Maubisse Formation south of the town of Maubisse. (C) Aitutu Formation south of Lei. (D) Lolotoi Complex east of Fahilacor.

discussed in the previous section on Geologic Setting, Aileu high-grade units contain detrital zircon ages of ca. 290 Ma, suggesting these sediments were sourced from the Sula Spur (Ely et al., 2014), similar to 254–358 Ma detrital zircons in Gondwana Sequence units (Zobell, 2007). The Aileu high-grade belt may therefore be a separate unit that collided with the Banda forearc prior to orogenesis at Timor (Ely et al., 2014), or it may have been part of the distal-most Australian margin during earliest orogenesis at Timor.

As in Tate et al. (2014), we use the division between the Aileu slate belt and the Aileu high-grade belt. The border between the two units is just south of Bazartete and Dare, with the high-grade belt following the north coast and

the slate belt extending south of Aileu and Letefoho (Fig. 4). We find that the Aileu high-grade belt exposes phyllite west of and into Dili, and amphibolite, schist, and marble to the east of Dili. Occasional gabbros with intrusive contacts are found along the full length of the high-grade belt close to the north coast. A body of peridotite is observed on the north coast of the Aileu high-grade belt close to Hilimanu, described in more detail by Berry (1981), Harris and Long (2000), and Falloon et al. (2006). The presence of gabbro intrusions and peridotite bodies within the Aileu high-grade belt supports the interpretation that this unit was originally located close to the ocean-continent transition. The Aileu slate belt consists largely of slate with occasional quartzite beds,

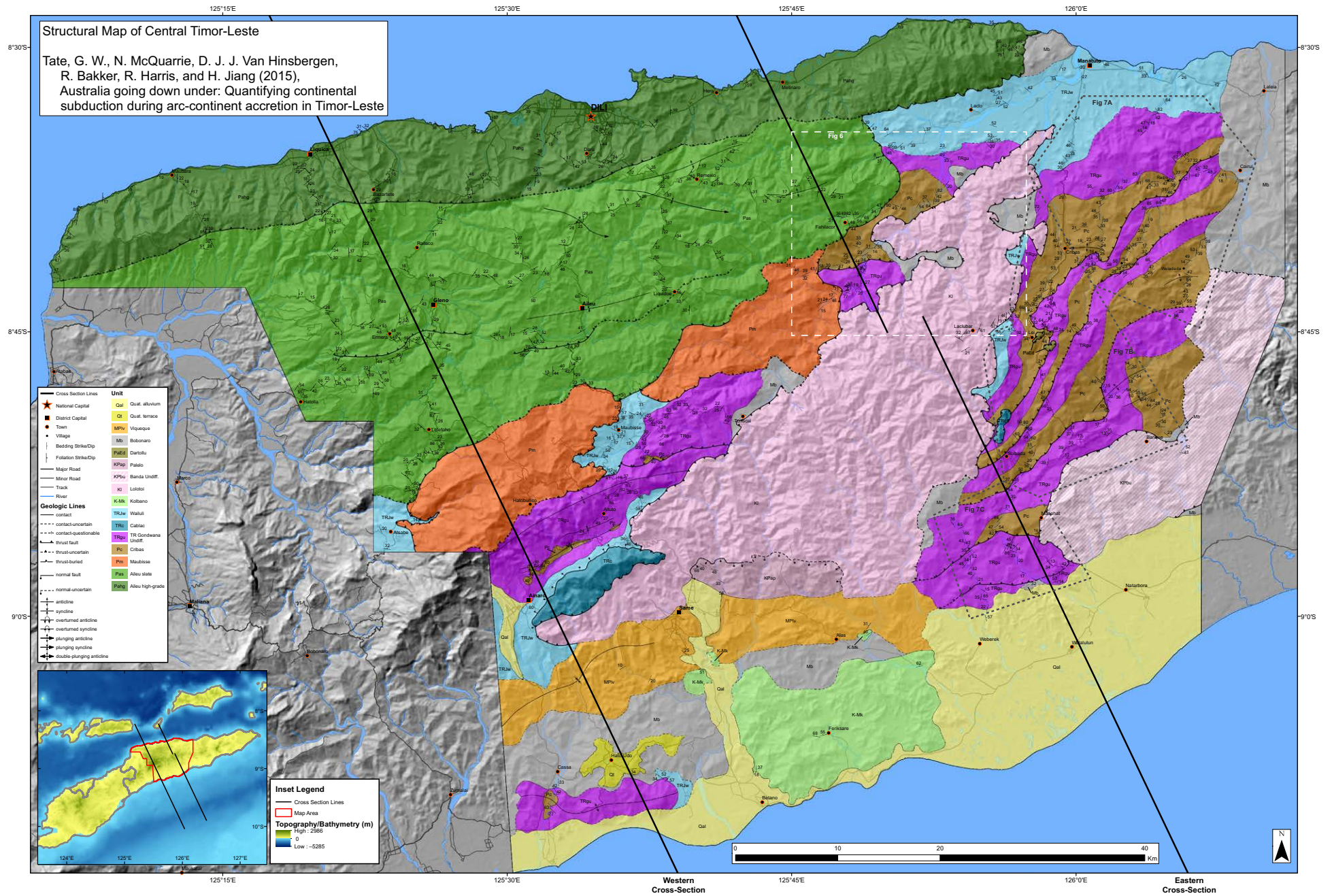


Figure 4. Structural map of central Timor-Leste. Location of Figure 6 indicated in dashed white. Bedding strike and dip data used in Figures 7A–7C indicated by dashed gray polygons.

transitioning from lowest grade metamorphism in the south to highest grade in the north. The southern portion of the Aileu slate belt on the road between the towns of Aileu and Maubisse bears strong lithologic similarity to both the Maubisse and Cribas formations, exposing mildly metamorphosed red-weathering fossiliferous limestones and interbedded metavolcanics along the road and a weakly metamorphosed sequence of black shales, ironstone nodules, and volcanoclastics just west of the road.

Aitutu Formation

Audley-Charles (1968) described the Aitutu Formation as being dominated by dense, very fine calcilutite and locally thin interbedded shales and calcareous shales. He noted the distinctive character of the Aitutu in outcrop, with the hard calcilutites forming prominent cliff faces and allowing little vegetation. Audley-Charles (1968) also estimated the thickness of the unit as 1 km thick and identified it as Triassic in age, unconformably deposited on the Permian Cribas Formation. We observe the Aitutu as containing consistently 10–15-cm-thick gray limestone beds that weather white with 5–10-cm-thick interbeds of shale (Fig. 3C). Limestone beds are usually free of macrofossils. Mapped thicknesses agree with the estimated thickness of 1 km by Audley-Charles (1968).

Niof and Babulu Formations

Contemporaneous with the Aitutu yet more prevalent in Indonesian West Timor are the Lower Triassic Niof and Upper Triassic Babulu Formations (Bird and Cook, 1991; Charlton et al., 2009). The lower half of the Niof Formation contains dark-gray shales with minor siltstones and sandstone, while the upper half contains red and green silty shales with occasional limestones (Bird and Cook, 1991). The Babulu Formation is dominated by well-bedded glauconitic sandstones, with some shales and subordinate limestones (Bird and Cook, 1991). We find the Niof and Babulu formations rarely exposed in our map area, and it appears the Triassic succession in Timor-Leste is dominated by the Aitutu Formation. The Niof Formation is found just northwest of Cribas and also south of Laclo; the Niof and Babulu formations are both exposed in a few locations just south of Raibu; and the Babulu Formation is exposed north of Weberek (Fig. 4). Additionally, the area immediately surrounding the town of Maubisse (identified as Triassic by Haig and McCartney [2010]) could be the Upper Triassic part of the Wailuli Formation or may instead belong to the Niof Formation.

Cablac Formation

The Cablac Formation consists of massive white calcilutite that weathers gray (Audley-Charles, 1968). It is observed most prominently at Mount Cablac just east of Ainaro and is also found in our map area north of Soibada. This

formation comprises many of the “Fatus” found across the island, which are isolated blocks of massive limestone several km in map extent with precipitous cliffs on every side. Originally dated as Miocene (and thus part of the Banda allochthon) (Audley-Charles, 1968), Haig et al. (2007) showed that the Cablac Formation is actually Upper Triassic to Lower Jurassic (and thus part of the para-autochthonous Gondwana Sequence).

Wailuli Formation

The Wailuli Formation was defined by Audley-Charles (1968) as a succession of blue-gray marls, micaceous shales, and some calcilutites with pebble conglomerates at the top of the unit. Estimated thickness ranges up to 1 km (Audley-Charles, 1968). Dated by Audley-Charles (1968) as Jurassic in age using ammonites and belemnites, Haig and McCartney (2010) use foraminifera to revise the age of the unit to Late Triassic to Jurassic. We observe the Wailuli Formation as fissile dark-gray shale weathering tan with intermittent siltstones and fine sandstones. Hillslopes of the Wailuli Formation commonly exhibit popcorn weathering. The stratigraphic transition from the Aitutu Formation to the Wailuli Formation is marked by five to ten 5-cm-thick gray calcarenites with fine tan shales interbedded, as exemplified just east of the town of Laclubar (Fig. 4).

Kolbano Sequence

The Australian passive margin sequence, the Kolbano Sequence, is dominated by massive calcilutites and also includes members of shales, cherts, and sandstones (Rosidi et al., 1979; Sawyer et al., 1993). These units would have been deposited within a proto-Banda embayment, the result of Jurassic rifting separating the Sula Spur of western New Guinea from modern northern Australia (Hall, 2002). The best exposure of the Kolbano Sequence is on the southern coast of West Timor around the town of Kolbano, where it is found as repeated thrust slices (Charlton et al., 1991; Sawyer et al., 1993; Harris, 2011). The units are similarly deformed in thrust slices in the Timor Sea, as visible with seismic data (Charlton et al., 1991; Sani et al., 1995). Similar exposures of the Kolbano Sequence are found on Rote Island just west of West Timor (Roosmawati and Harris, 2009). While ages of the full sequence observed in West Timor range from Late Jurassic to early Pliocene (Rosidi et al., 1979; Sawyer et al., 1993), ages in East Timor are predominantly Cretaceous (Audley-Charles, 1968), and the youngest member is late Miocene (ca. 9.8 Ma) in age (Keep and Haig, 2010). The stratigraphic thickness of the full Kolbano Sequence in Timor-Leste is ~500 m (Haig and McCartney, 2007). In our map area, we observe Kolbano Sequence units only in sparse outcrops southeast of Same. This region exposes the Cretaceous Wai Bua Formation of Audley-Charles (1968), consisting of chalky pink limestone weathering white and black.

Banda Terrane

Lolotoi Complex

Allochthonous units on Timor derived from the Banda forearc can be divided into metamorphic forearc basement and the overlying sedimentary and volcanic cover units (Harris, 2006). The metamorphic forearc basement, known in East Timor as the Lolotoi Complex (Audley-Charles, 1968), was described by Standley and Harris (2009) to contain greenschist- to amphibolite-facies metasediments and meta-igneous units including graphitic phyllite, garnet-bearing quartz-mica schist, and amphibolite gneiss. We observe the Lolotoi Complex as heavily chloritized pelites, basalts, and volcanoclastics ranging from greenschist to amphibolite facies (Fig. 3D). Although some authors have suggested that the Lolotoi Complex is Australian basement (Charlton, 2002) or more strongly metamorphosed Aileu Complex (Kaneko et al., 2007), young detrital zircons (<40 Ma) found within the Lolotoi Complex (Harris, 2006; Standley and Harris, 2009) confirm earlier hypotheses (Audley-Charles, 1968) that the Lolotoi Complex is the allochthonous forearc of the Banda volcanic arc and is of Asian affinity. Previous thermochronologic studies suggest cooling of the Mutis Complex (the Lolotoi Complex equivalent in West Timor) through hornblende and mica $^{40}\text{Ar}/^{39}\text{Ar}$ closure between 31 and 38 Ma (Harris, 2006) and cooling of the Lolotoi Complex at the town of Laclubar (Fig. 4) through zircon (U-Th)/He closure at 25.7 ± 1.5 Ma (Tate et al., 2014). This cooling history, coupled with the presence of unmetamorphosed sedimentary units deposited unconformably on the metamorphic Lolotoi Complex prior to the Miocene (Audley-Charles, 1968), suggests significant exhumation in this portion of the Banda forearc prior to collision at Timor.

Banda Terrane Sedimentary and Volcanic Cover Units

Also attributed to the Banda Terrane and preserved in unconformable contact with the Lolotoi Complex are units of Banda forearc sedimentary and volcanic cover, including the Middle-Upper Cretaceous to Paleocene Palelo Group, the Paleocene–Eocene Dartollu Limestone, the Eocene–Oligocene Barique Formation, and the Miocene–Pliocene Manamas Formation (Harris, 2006) (Fig. 2). Northeast of the town of Same, we observe the Palelo Group, containing sections of stacked limestone beds, conglomerates, and occasional basalts. In the area around the town of Barique, the Barique Formation is exposed as volcanic conglomerates and lavas. The Dartollu Limestone is observed in isolated exposures as limestone klippen above the Gondwana Sequence thrust stack, such as just east of Laclubar. We have not mapped the Banda Terrane in detail. For instance, around the town of Barique, the contact between the Barique Formation and the Lolotoi Complex is not mapped, and in this location, we indicate only undifferentiated Banda Terrane in Figure 4.

Banda Orogen Sequence

Roosmawati and Harris (2009) define the Banda Orogen Sequence as consisting of units that have formed or been deposited since the start of collision of the continental margin with the Banda forearc at Timor.

Bobonaro Mélange

The Bobonaro mélange is a tectonic mélange found throughout Timor in structural contact above units of Australian affinity and below the Banda Terrane (Harris et al., 1998). Originally identified as an olistostrome (Audley-Charles, 1968), Harris et al. (1998) interpreted this unit as a tectonic mélange associated with the obduction of the Banda forearc onto the Australian margin. The Bobonaro mélange contains blocks of all of the stratigraphic units on Timor, as well as serpentinites and metaigneous rocks, surrounded by a clay matrix sourced mostly from the Wailuli Formation (Harris et al., 1998). The Bobonaro mélange is interpreted as the source of mud volcanoes in West Timor and is visible through seismic data as mud diapirs offshore in the Timor Sea and the Savu Sea (Harris et al., 1998). Maximum documented thickness is ~2 km (Audley-Charles, 1968). We have observed the Bobonaro mélange in several areas between the Gondwana Sequence units and the Banda Terrane, such as near the town of Barique, west of the town of Cribas, and around and south of Laleia (Fig. 4). In these areas, blocks of the Aitutu Formation, Lolotoi Complex, and ultramafics are found on the scale of several meters to a few kilometers, surrounded by a fine-grained tan-weathering shale matrix identical in lithologic character to the Wailuli Formation. Occasionally 5–10-cm-long gypsum crystals are found within the shale matrix. In some locales, such as south of Maubisse and Turiscai or east of Laclubar, a thin zone of cm- to m-scale thickness of highly deformed shale is present between the Banda Terrane and Gondwana Sequence, without the inclusion of exotic blocks.

Viqueque Sequence

The Viqueque Sequence consists of deepwater sedimentary rocks that are the earliest synorogenic deposits on Timor spanning 5.6 to ca. 3 Ma (Audley-Charles, 1968, 1986; Haig and McCartain, 2007; Aben et al., 2014; Tate et al., 2014). This sequence consists of a basal unit of chalky limestones and marls, overlain by a coarsening-upward sequence of clays and turbidites (Haig and McCartain, 2007; Tate et al., 2014). Basal limestones are deposited unconformably on the Bobonaro mélange with no intervening Banda Terrane or Kolbano Sequence in their normal structural position, indicating gravitational sliding and submarine removal of these units prior to basal Viqueque Sequence deposition (Tate et al., 2014). Our map area contains one basin of the Viqueque Sequence, located in the southern map area near Same and Alas. We observe the Viqueque Sequence deposited unconformably on the Bobonaro mélange

in several locations in this basin. In other locations along the southern margins of the basin, the Viqueque Sequence is observed unconformably over the Kolbano Sequence, and in one location east of Same, the northern margin of the basin is observed to overlie units of the Banda Terrane. Other contacts of the Viqueque Sequence with the Banda Terrane are inferred from aerial photography and previous mapping (Audley-Charles, 1968).

Younger Synorogenics

The youngest synorogenic deposits of the Banda Orogen Sequence include coral terraces and alluvial gravels (Audley-Charles, 1968; Roosmawati and Harris, 2009). These units are found most extensively in the southern map area, with wide coral terrace exposure near Hatudo and extensive Quaternary alluvium along the south coast extending farther inland in the southeast map area than in the southwest. In the north map area, these Quaternary synorogenics are much smaller in extent, with alluvial deposits constrained to river valleys and isolated coral terraces east of Manatuto less than 1 km in diameter. Uranium-series dating of coral terraces by Cox (2009) yielded ages ranging from 1.85 ± 0.05 ka to 146.7 ± 1.1 ka. Mapping of these terraces and others suggests surface uplift of 0.2–0.5 mm/yr near Manatuto, with faster uplift rates up to 1.6 mm/yr east of our map area, over the past 150–500 k.y. (Cox, 2009). Tate et al. (2014) found that apatite (U-Th)/He ages from Gondwana Sequence units at Manatuto suggest similar exhumation rates of 0.28–0.52 mm/yr.

CONODONT PALEONTOLOGY

In a number of areas, lithostratigraphic identification of Gondwana Sequence units is very difficult. Conodont paleontology was employed where possible to aid stratigraphic correlation. Several shale and limestone units within the Gondwana Sequence were sampled for conodont paleontology, and ages determined with these samples have provided additional constraints for our mapping. Shale samples were broken by sodium hydrosulfite solution (10%) and hydrogen peroxide (10%) successively. Limestone samples were crushed into 1-cm³-size fragments and dissolved with dilute acetic acid (10%);

2.80–2.81 g/ml gravity liquid made of bromoform and acetone was used in conodont separation for all the samples.

Of the samples processed, those containing conodonts are listed in Table 1. These samples contain Middle to Upper Triassic conodonts. One sample contains the Anisian species *Gladigondolella tethydis* and *Neogondolella* sp., one contains upper Carnian *Carniepigondolella orchardi*, one contains lower Norian *Norigondolella navicular*, and three others contain lower Carnian *Metapolygnathus polygnathiformis* (Orchard, 2010). In several locations, these ages revised our stratigraphic correlation from Permian to Triassic units.

STRUCTURAL MAPPING

Previous Mapping

Previous mapping in East Timor was largely reconnaissance in nature or narrow in geographic extent. Mapping by Audley-Charles (1968) has remained the most frequently used regional map, despite the fact that much of it was completed as a reconnaissance map or using only aerial photographs. Upon inspection, several problems are apparent with the Audley-Charles 1968 map, most notably in relation to the Gondwana Sequence. Audley-Charles (1968) mapped Gondwana Sequence exposures in our eastern map area between Manatuto and Barique as one double-plunging anticline striking east-west. As mapped by Audley-Charles (1968), this anticline is cored with Cribas and Atahoc formations and has dipping limbs exposing the Aitutu and Wailuli formations to the north and south. This is problematic for two reasons: (1) the strikes of units mapped by Audley-Charles in this area are predominantly NNE, generally 45°–90° oblique to the trend of mapped contacts; and (2) the ~40° dip of these measurements, when combined with the ~20-km-wide exposure of Cribas-Wailuli units, would imply a total stratigraphic Cribas-Wailuli thickness of ~12 km. This is contrary to the observed thicknesses of 1 km each for the Cribas, Aitutu, and Wailuli formations both on Timor (Audley-Charles, 1968) and in seismic sections south of the Timor Trough (Snyder et al., 1996). Zobell (2007) observed units in this region striking predominantly NNE and noted repeating lithologies that suggested the Gondwana Sequence is structurally repeated as a duplex in this region instead of deformed as a single anticline.

TABLE 1. SAMPLES CONTAINING CONODONTS, SPECIES FOUND, AND CORRESPONDING AGES

Sample	Latitude	Longitude	Species	Age
TL10-92	–8.525735	126.00511	<i>Metapolygnathus polygnathiformis</i> (one specimen)	Lower Carnian
TL10-188	–8.823945	125.707079	<i>Metapolygnathus polygnathiformis</i> (one specimen)	Lower Carnian
TL11-02	–8.52022	126.0575	<i>Gladigondolella tethydis</i> , <i>Neogondolella</i> sp.	Anisian
TL11-16	–8.614584	126.08451	<i>Metapolygnathus polygnathiformis</i>	Lower Carnian
TL11-189	–8.937763	125.905258	<i>Carniepigondolella orchardi</i>	Upper Carnian
TL11-379	–8.543646	125.930933	<i>Norigondolella navicular</i>	Lower Norian

Note: Ages from Orchard (2010).

Several other studies were used when completing our mapping. Contacts with the Banda Terrane of the massif centered around Laclubar, Turisca, and Same were drawn using mapping by Standley and Harris (2009) and Grady and Berry (1977). Foraminiferal dating by Haig and McCartain (2010) was used to identify units in the area around Maubisse as Late Triassic in age and also to confirm areas we independently mapped as Triassic Gondwana Sequence. Foraminiferal dating in McCartain et al. (2006) is used to refine our field mapping of the Cribas Formation between the towns of Aitutu and Ainaro. Aerial photography was also used to map the edges of the Lolotoi Complex and for dashed contacts and thrust faults throughout the map.

Mapping Methods

Field mapping was conducted using 1:50,000-scale topographic maps from Bakosurtanal, Indonesia as base maps. Global positioning system was used for location in the World Geodetic System (WGS) 1984 reference frame. Mapping focused on exposures of the Gondwana Sequence and Aileu Complex, documenting structural contacts with units of the Banda Terrane but few characteristics within the Banda units. Each region of focus was mapped as follows: (1) The eastern map area (the district of Manatuto) was mapped almost entirely using hikes through rivers, with exposure varying from continuous to outcrops every few hundred meters. Observations were also taken every few hundred meters where road cuts were available on the road from Manatuto to Natarbora and alongside roads to Laclubar, Soibada, and Barique. (2) Mapping in the Ainaro-Maubisse-Turisca area (northern Ainaro district) was primarily conducted using observations at road cuts every few hundred meters. River traverses in the Maubisse area were used as well, with exposure varying from continuous to outcrops every few hundred meters. (3) Mapping along the south coast near Same, Alas, and Hatudo (southern Ainaro and southern Manufahi districts) was conducted almost entirely using river traverses. Low relief and dense vegetation led to limited exposure, with exposure intervals every few hundred meters at best. (4) Mapping in the northern map area (Dili, Aileu, Liquiçá, and Ermera districts) was conducted almost entirely using the relatively extensive road network. Observations were taken every few hundred meters. River hikes supplemented our observations near Dili and southwest of Aileu, with exposure varying from continuous to outcrops every few hundred meters.

New Mapping

Our new structural map of central East Timor is presented in Figure 4. Directly apparent in our new mapping is the structural repetition of Gondwana Sequence units. The Permian–Triassic stratigraphy of the Gondwana Sequence is repeated by a series of thrust faults in both the eastern and western map area. Additional deformation within Australian-affinity units is documented in the Aileu Complex, with several mapped thrusts placed at boundaries of lith-

ology and metamorphic grade. The mapped position of Banda Terrane units relative to deformed Gondwana Sequence units requires a thrust relationship of the Banda Terrane over the Gondwana Sequence, with Bobonaro mélange mapped between them. This broad map pattern is consistent with the interpretation that Timor has developed as a duplex of Australian-affinity units below an overthrust Banda forearc klippe.

Eastern Map Area

The eastern map area is dominated by structural repetition of the Gondwana Sequence between the towns of Manatuto and Natarbora. Thrust faults are observed repeating the Permian–Triassic stratigraphy, with units striking predominantly NNE and dipping WNW. This thrust repetition is exposed in a window through the overthrust Banda klippe, with exposures of the Banda thrust sheet both east and west of this window. Field observations provide strong evidence of faulting where stratigraphic order is broken (Fig. 5). Significant internal deformation is visible at the base of the Cribas Formation proximal to faults that place Cribas over Aitutu. In these locations, shale and siltstone beds are heavily folded and limestone beds within the Cribas Formation are commonly boudinaged. Deformation within the Aitutu Formation near faults is also apparent, with beds dipping opposite to the regional orientation within ~100 m of the fault location (forming apparent footwall synclines) or extensive chevron folding of limestone beds near Cairui and Manehat. A hot spring including oil seepage is coincident with the Aitutu-over-Aitutu thrust fault just north of Weberek.

This area was previously mapped as a double-plunging anticline striking east-west (Audley-Charles, 1968). Our observed strikes and dips are consistent with those indicated by Audley-Charles (1968), although as we have noted above, these strikes are nearly perpendicular to mapped contacts by Audley-Charles (1968). In the location of the previously mapped Permian-cored anticline at the town of Cribas (Audley-Charles, 1968), we find an anticline of the Cribas Formation in the hanging wall of a fault and Aitutu Formation in the footwall that is south-dipping within 100 m of the fault. This forms an apparent hanging-wall anticline–footwall syncline pair; while farther south, the Aitutu Formation returns to a northwest dip, and the Cribas Formation can be found repeated again stratigraphically below that same exposure of the Aitutu.

Also within the eastern half of our map area but just northwest of the central Banda klippe, thrust repetition of Australian-affinity units is documented near the town of Fahilacor (detail in Fig. 6). Exposure of the Cribas and Aitutu formations was previously undocumented near Fahilacor, where only undifferentiated Gondwana Sequence (Grady and Berry, 1977) or a triple-junction between Maubisse Formation, Aileu Complex, and Lolotoi Complex (Audley-Charles, 1968) was mapped previously. We map one thrust of Cribas Formation over Aitutu Formation, with extensive chevron folding within the Aitutu Formation in the footwall of this fault (Fig. 5C) and a hot spring and hydrothermal alteration of the Aitutu Formation coincident with the fault location. The Maubisse Formation is thrust over both the Cribas and Aitutu formations, and the Aileu

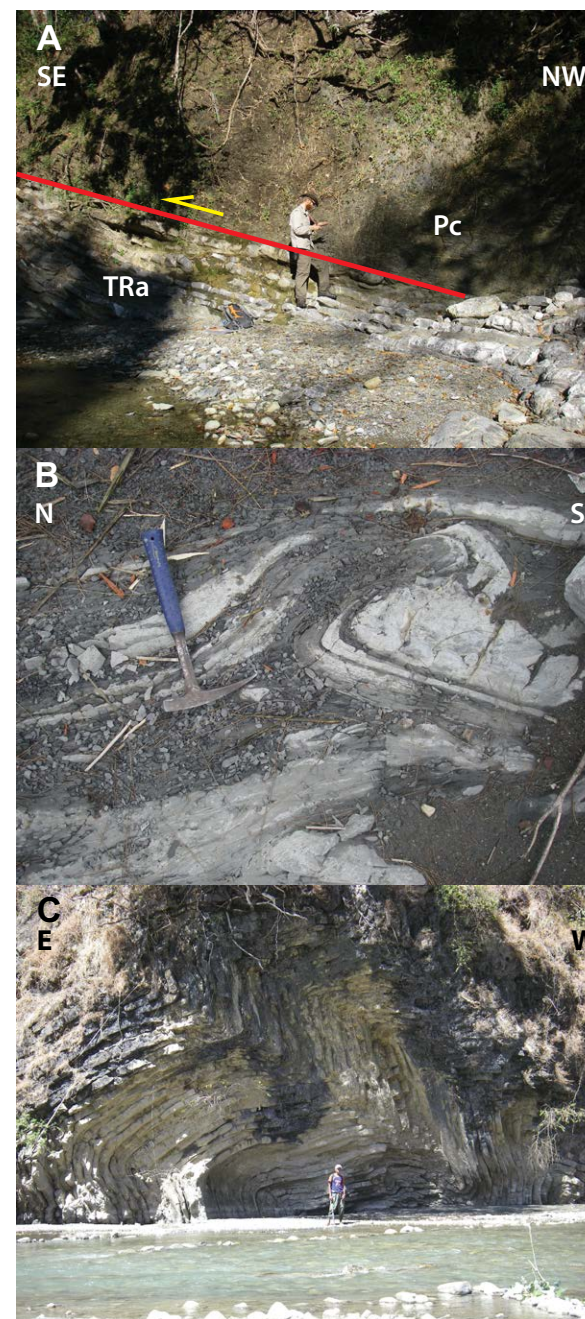
Figure 5. Field examples of structural trends within the Gondwana Sequence duplex. (A) Thrusting of Permian Cribas Formation (Pc) over Triassic Aitutu Formation (TRa) south of the town of Tuquetti. (B) South-vergent folds in the lower Cribas Formation southwest of the town of Cribas. (C) Chevron folds in the Aitutu Formation within the footwall of a Maubisse-over-Aitutu thrust fault south of Fahilacor.

Complex and Lolotoi Complex are thrust over the Cribas, Aitutu, and Maubisse formations. The structural relation between the Lolotoi and Aileu complexes is not observed at the surface.

Our mapping also indicates key systematic shifts in the regional trends of the repeated units in the eastern window. First, we note that on the eastern and southwestern ends of the eastern window (as well as outside the eastern window) the dominant strike of Gondwana Sequence units is ENE (Figs. 7A and 7C), whereas between Soibada and Cribas, this strike shifts to NNE (Fig. 7B). Second, units dip much more steeply near Soibada and Cribas (dips $\sim 45^\circ$; see Fig. 7B) compared to southern areas west of Manehat (scattered dips approximating 25° ; see Fig. 7C). Third, the repeated package is folded just north of Barique, with an anticline folding one of the thrusts of Cribas Formation over Aitutu Formation. This folded thrust fault and change in the dip of repeated units suggest a late stage of deformation that has refolded the repeated units, which could be the same mechanism that controls the shift from ENE to NNE strikes.

Map patterns in the eastern map area are interpreted to represent duplexing of the Permian and Triassic Gondwana Sequence stratigraphy below the overthrust Banda forearc. For example, Figure 6 shows the fault contact between the Lolotoi Complex and Gondwana Sequence to the south, east, and northeast of Fahilacor approximately following topographic contours. Mapped windows through the Lolotoi Complex are separated by as little 2.5–5 km. These observations require the mapped faults on all sides of the Lolotoi Complex to be low angle and merge at a shallow depth, suggesting a single low-angle thrust below what we map as the Lolotoi klippe. Additionally, Figures 4 and 6 show Gondwana Sequence units to the east of Laclubar dipping 32° – 73° west and northwest toward Lolotoi Complex exposures, suggesting a position structurally below the Lolotoi Complex with a much steeper Lolotoi over Gondwana Sequence relationship. We interpret this steeply west- and northwest-dipping fault to be an originally low-angle thrust that has been rotated to a steep angle during folding of the Banda forearc nappe due to duplexing of the Gondwana Sequence.

The shifting trends of units and folded faults within the duplex in the eastern window suggest a late stage of deformation after initial duplex development. We suggest that the southern transition from regions of the duplex dipping 45° to regions dipping 25° and the fold of the duplex fault near Barique are coincident with a ramp-flat transition where the duplex is moving over a sub-surface ramp. The shift in duplex strike from ENE to NNE may either represent (1) motion of a duplex of constant thickness over an oblique segment of this ramp or (2) the lateral margin of an antiformal stack that has thrust over a straight ramp. Either of these possibilities would allow for duplexed units to strike NNE despite a constant transport direction to the SSE.



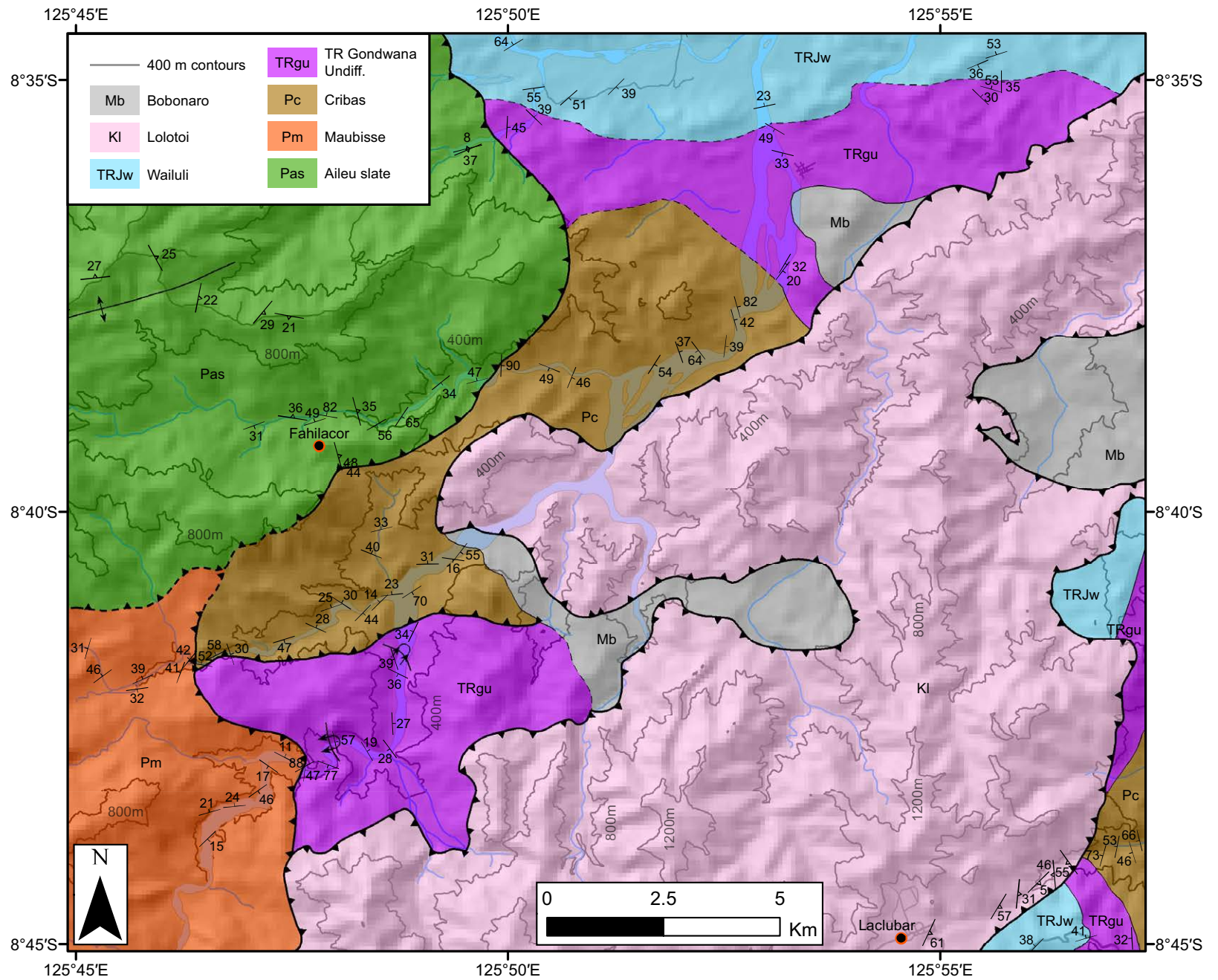


Figure 6. Detailed structural map of Fahilacor area. Map symbols used as in Figure 4. Elevation contours with 400 m contour interval are included.

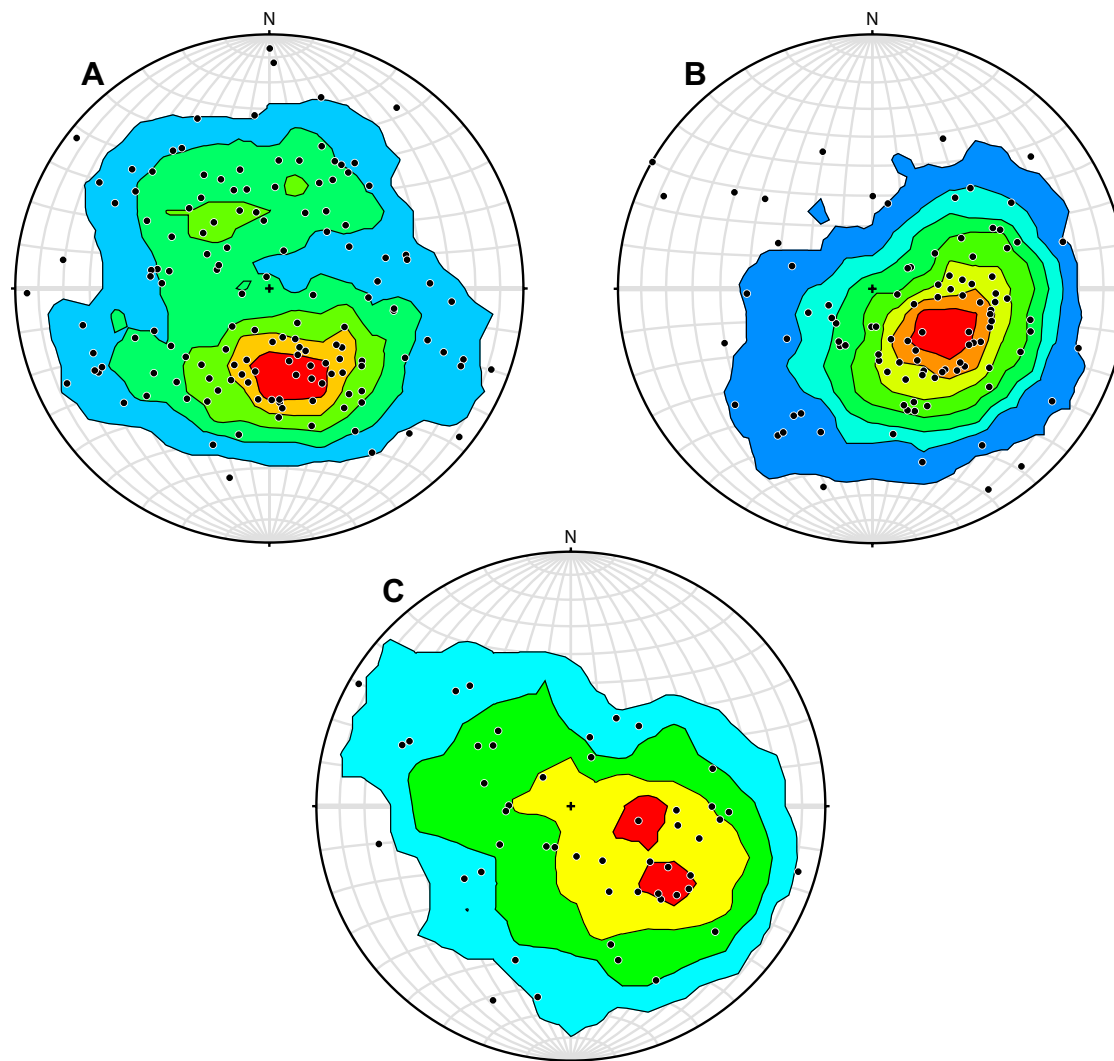


Figure 7. Equal-area stereonet plots of poles to bedding planes for Permian, Triassic, and Jurassic Gondwana Sequence units in three regions in the eastern map area; locations marked in Figure 4. (A) Tuquetti-Raibu area, $n = 142$; (B) Soibada-Lei area, $n = 101$; and (C) area west of Manehat, $n = 49$. Contouring with Kamb method, interval = 2 sigma and significance = 3 sigma. Stereonet 9 was used to create these plots (Allmendinger et al., 2013; Cardozo and Allmendinger, 2013).

The map pattern showing terminations of stratigraphic contacts and duplex thrusts against Banda klippen and the Bobonaro mélangé suggests significant subduction erosion of the Gondwana duplex along the thrust boundary between that duplex and the Banda Terrane. This subduction erosion likely provides the blocks of Gondwana Sequence units present within the Bobonaro mélangé. Erosion of duplex faults along the upper décollement also implies some out-of-sequence motion along the upper décollement since duplex formation.

Central Western and Southwestern Map Area

The central western map area between Atsabe and Turiscai is dominated by Gondwana Sequence units at the highest elevations of the island (peaking at over 2900 m). The WSW to ENE trend of exposed Gondwana Sequence rocks from the towns of Ainaro to Aituto to Turiscai was previously mapped as a single anticline exposing only the Aitutu Formation at the surface

(Audley-Charles, 1968). Our map pattern near Aitutu is also dominated by an anticline of Aitutu Formation, although folds in the southern limb of this anticline expose the Cribas Formation that is stratigraphically below this Aitutu Formation. Exposure of the Cribas Formation in the valley south of the town of Aitutu is confirmed by previous dating of foraminifera (McCartain et al., 2006). We also map a thrust fault on the north limb of this anticline just south of the town of Maubisse, which exposes a portion of the Cribas Formation in its hanging wall. The broad region of high topography and exposed Gondwana Sequence rocks is much wider than any single structure (individual anticlines or faults) and is associated with young (ca. 2 Ma) apatite (U-Th)/He cooling ages (Tate et al., 2014). Along the northern boundary of the Aitutu anticline, a thrust fault is mapped that places the Maubisse Formation over the Aitutu Formation. The thrust at the base of the Maubisse Formation is most clearly shown to have a low angle near the town of Maubisse, where this fault approximately follows topography above units dated as Triassic around the town of Maubisse proper (Haig and McCartain 2010). Additionally, a low-angle thrust fault that dips north and has a top to the south displacement was mapped between Maubisse Formation limestones and the underlying Wailuli Formation just east of Atsabe. This fault is exposed in several locations on both sides of the river valley. A separate low-angle thrust is mapped along the road between the towns of Aileu and Maubisse that places the Aileu slate belt above the Maubisse Formation.

The Cribas and Aitutu formations are also mapped near the south coast (south of Hatudo), where they were not previously documented. Audley-Charles (1968) mapped scattered exposures of the Wailuli Formation surrounded by Bobonaro mélange, while we find an east-west–striking anticline plunging east exposing the Cribas, Aitutu, and Wailuli formations at the surface.

These areas of the western map area also support the interpretation that Permian–Triassic Gondwana Sequence units have developed as a duplex below the Banda Terrane. This western region appears to expose a shallower level of the duplex than the eastern map area, because it is dominated by several large anticlines of the Aitutu Formation, and the stratigraphically deeper Cribas Formation is only exposed in a few isolated locations. The restriction of Maubisse Formation horses to the most northwesterly portions of the Gondwana Sequence duplex supports the interpretation that this unit was restricted to the more northerly portions of the pre-collisional margin.

Northwest Map Area: Aileu Complex

Our mapping also documents and supports previous interpretations of internal deformation within the Aileu Complex (Berry and Grady, 1981; Prasetyadi and Harris, 1996). However, our main goal was not to describe the penetrative deformation but to document large-scale map structures that repeat stratigraphy. A thrust fault is mapped in the southern Aileu slate belt 3 km south of the town of Aileu where slates with rare quartzites are thrust over lower-grade slates interbedded with lightly metamorphosed fossiliferous

Maubisse limestones and several protoliths similar to the Cribas Formation (black shales, iron siltstones, red and green volcanoclastics, and occasional sandstones). Two other thrust faults are mapped at transitions of metamorphic grade. The first is between greenschist- to amphibolite-grade Aileu high-grade belt units along the north coast and the lower-grade Aileu slate belt, a fault that runs 2 km south of Dare. The second is 3 km south of Gleno, with higher-grade slates containing visible micas thrust over very lightly metamorphosed slates to the south. Other faults have been difficult to map within the Aileu slate belt due to the fairly monotonous lithologies of slate and occasional quartzite. Instead, broad patterns of anticlines and synclines are evident.

This map pattern is suggestive of thrust stacking within the Aileu Complex. The spacing between mapped thrusts suggests that either a thicker stratigraphic package is repeated in the Aileu Complex than in the unmetamorphosed Gondwana Sequence or that some thrusts marking stratigraphic repetition remain unmapped. A broad pattern of folding is found in portions of the Aileu Complex, for instance around the towns of Remexio and Aileu (Fig. 4). These broad folds may have formed during thrust repetition of the slate belt or during a later stage of subsurface deformation.

■ **BALANCED CROSS SECTIONS**

Methods

Two balanced cross sections (Figs. 8 and 9) were constructed through our map area, extending from the Banda arc to the Timor Trough. The western section was drawn along the trend of the towns of Liquiçá and Ainaro. The eastern section was drawn parallel to the western section, along the trend of Metinaro to Fahilacor and Soibada to west of Natarbora and containing a break with an along-strike shift in the section west of Laclubar in the exposure of the Lolotoi Complex. Although oblique to the modern GPS convergence vectors (Fig. 1), both of the cross sections are perpendicular to the structural trend of units they intersect on the surface as well as to the Timor Trough. Additionally, although duplexed units just east of the eastern section near Soibada are oblique to the section trend, we have noted above that this NNE strike is likely due to a subsurface ramp, whereas motion of material likely remains consistently SSE. Original sections were drawn by hand at a scale of 1:200,000. Surface exposure is constrained by map patterns and measured strike and dip data, though small-scale folding and faulting within units (such as the meter-scale deformation common near duplex faults) is not represented. Line length of each thrust sheet and horse was matched on the deformed and restored cross sections. The restored lengths of the Cribas and Aitutu formations are the same as the restored length of the Kolbano Sequence, whereas the Maubisse Formation and Aileu Complex restore as more distal units on the Australian margin. Faulting and folding were drawn using the kink methods of Suppe (1983).

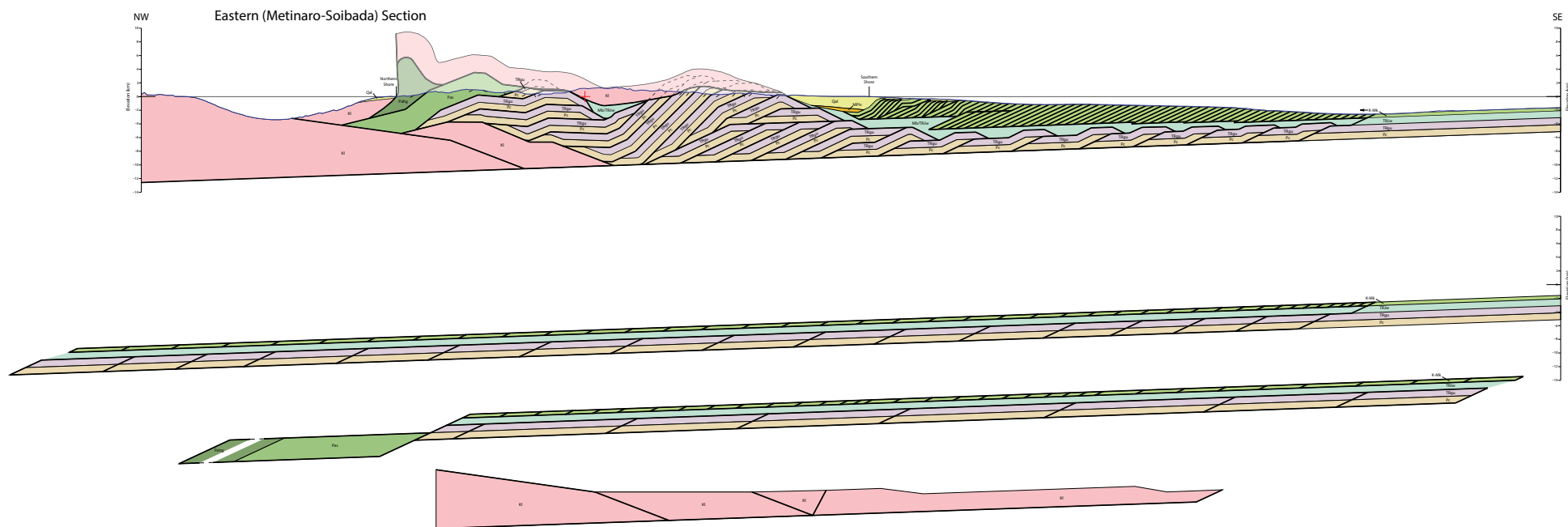


Figure 8. Eastern balanced cross section and restored section. No vertical exaggeration. Bold lines indicate faults; thin lines indicate stratigraphic contacts. Upper section: deformed section. Lower three sections: broken restored section (lowest is northwestern part of restored section; middle is central part of restored section; upper is southeastern part of restored section). In deformed section, section break at red cross.

Cross Section Constraints

Thicknesses for each unit correspond to those discussed above: 1 km each for the Maubisse, Cribas, and Aitutu formations, and 0.5 km for the Kolbano Sequence. Difficulty constraining stratigraphic repetition in the Aileu Complex leads us to use maximum thicknesses for Aileu horses. No attempt is made to preserve the thickness of the Wailuli Formation in these cross sections because it acts as the matrix of the Bobonaro mélangé, which has highly variable thickness and is incorporated within mud volcanoes both onshore and offshore (Harris et al., 1998).

Orogenic wedge geometry is constrained by the topographic and bathymetric surface and the shape of the basal décollement. Topography and bathymetry data were obtained from Smith and Sandwell (1997). The geometry of deformation within ~10 km of the Timor Trough and the thickness of sedimentary units on the Australian shelf (~3.3 km) is based on seismic and well data presented in Snyder et al. (1996). Moho depth is constrained to be 35–40 km below the Australian shelf and 45–50 km below Timor based on seismic reflection data (Richardson and Blundell, 1996). The thickness of the

wedge of mostly sedimentary units at the highest point of the orogen is from Shulgin et al. (2009), who use seismic refraction to model a 10–12 km package of sedimentary densities just to the west of the island of Savu. The surface geology of Savu is a narrow fold-thrust belt of Gondwana Sequence units similar to those mapped on Timor (Harris et al., 2009). The agreement between the change in Moho depth and the thickness estimate for the wedge of sedimentary units together (1) suggest that Australian basement rocks below Permian strata are not incorporated within the orogen and (2) constrain our use of a 2° décollement in these cross sections. Our wedge geometry also incorporates backthrusting along the northern side of Timor, supported both by seismic sections just east of Timor (Snyder et al., 1996) and by wells on the northern side of Savu just west of Timor (Harris, 2011).

Thermochronologic constraints for the timing of deformation on Timor are incorporated into the sequence of deformation implied by these cross sections. On the southern slopes of the eastern window in the same location as the folded duplex thrust fault north of Barique, apatite (U-Th)/He data transition from northwest to southeast from 2.0 ± 0.6 Ma to 4.9 ± 0.9 Ma and indicate a spatial change in exhumation rate (Tate et al., 2014). A sharp

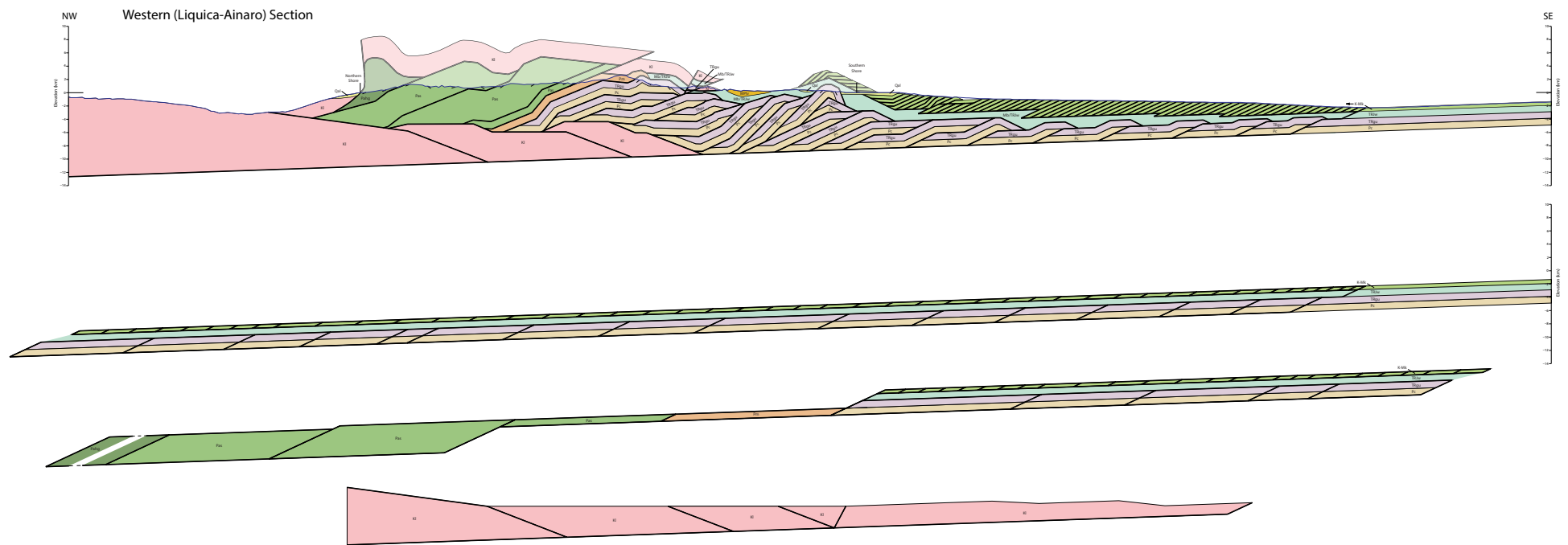


Figure 9. Western balanced cross section and restored section. No vertical exaggeration. Bold lines indicate faults; thin lines indicate stratigraphic contacts. Upper section: deformed section. Lower three sections: broken restored section (lowest is northwestern part of restored section; middle is central part of restored section; upper is southeastern part of restored section).

boundary in exhumation magnitude coincides with the thrust separating the Aileu slate belt and the Maubisse Formation, with significantly more exhumation in the Aileu slate belt as demonstrated by discontinuities in apatite and zircon (U-Th)/He (Tate et al., 2014), apatite fission track (Harris et al., 2000; Tate et al., 2014), and vitrinite reflectance (Harris et al., 2000). Additionally, a mechanism for exhumation of 2.7–4.6 km of material since 1.5–1.8 Ma is required in the western Aileu slate belt as indicated by zircon (U-Th)/He data (Tate et al., 2014).

Cross Section Interpretations

The cross sections presented here (Figs. 8 and 9) follow our map pattern interpretation that Timor has deformed as a duplex of pre-Jurassic Australian-affinity strata below an overthrust sheet of the Banda forearc. The majority of the wedge is filled with duplexed Permian–Jurassic stratigraphy, while the Wailuli Formation and Bobonaro mélange act as an upper décollement between this duplex and the Banda Terrane.

Deformation of the Kolbano Sequence is entirely in the foreland. Following sandbox models and cross sections in Harris (2006), a fold-thrust belt of Kolbano Sequence thrust sheets with total length equal to the Cribas-Aitutu duplex was constructed in front of the leading edge of the Banda Terrane klippe above the Wailuli Formation–Bobonaro mélange upper décollement. In the eastern cross section, this Kolbano fold-thrust belt is still buried below Quaternary alluvium; in between the two cross-section lines, the Kolbano Sequence is exposed and mapped at the surface; and at the western cross section, the Kolbano Sequence has been eroded from above the Gondwana Sequence anticline at the south coast. Not only does the map pattern suggest erosion of the Kolbano Sequence in the western section south of Hatudo, but apatite (U-Th)/He data from the Wailuli Formation at this location require removal of 1–2 km of material (Tate et al., 2014), matching the thickness of the eroded Kolbano fold-thrust belt drawn in the western section.

The cross sections presented here highlight locations where Banda Terrane and Kolbano Sequence units were removed from above the Bobonaro mélange via slumping, exhuming this mélange to the sea floor long before emergence of Timor, as suggested by Tate et al. (2014). Those authors note

that the Viqueque deepwater synorogenics were unconformably deposited directly on the Bobonaro mélange of the upper décollement with neither the Banda Terrane nor the Kolbano Sequence intervening. Tate et al. (2014) therefore suggested that duplexing of the Gondwana Sequence caused gravitational sliding (slumping) of the Kolbano Sequence and Banda Terrane along the Bobonaro mélange, which created the basins that preserve the Viqueque Sequence today. We similarly incorporate slumping along the north coast of Timor to accommodate the exhumation of Aileu high-grade units through muscovite $^{40}\text{Ar}/^{39}\text{Ar}$ closure at 7.1 ± 0.3 Ma before emergence above sea level, as suggested in Tate et al. (2014).

A number of geometries have been included in these cross sections to match thermochronologic constraints from Tate et al. (2014). Out-of-sequence motion along foreland ramps near the south coast in both the eastern and western cross sections move horses of the Cribas-Aitutu duplex over other horses farther to the foreland, matching patterns of late folding of the duplex while allowing for a mechanism of cooling through apatite (U-Th)/He closure at ca. 2 Ma. The thrust fault between the Aileu slate belt and the Maubisse Formation in the western cross section is drawn as an out-of-sequence thrust with 3.1 km of displacement to follow the observed discontinuity in exhumation magnitude. Lastly, backthrusting of the Aileu and Cribas-Aitutu duplex over the Banda forearc and subsequent duplexing of the underthrust Banda forearc allows a mechanism for cooling of the Aileu Complex through zircon (U-Th)/He closure at 1.5–4.4 Ma and for cooling of Gondwana Sequence units near Ainaro through apatite (U-Th)/He closure at 1.8–2.8 Ma.

Geometries of the Gondwana Sequence duplex in the southern offshore portion of the section are less constrained than onshore where surface mapping exists. For instance, Figure 10 shows one possible alternative geometry for the southern offshore portion of the western section. This alternative geometry has the same shortening amount and undeformed length as the geometry in Figure 9, yet redistributes the shortening for a possible case where (1) more shortening

has occurred in the hinterland and less in the foreland and (2) the frontal ramp within the Permian–Triassic section is not as close to the Timor Trough as in the seismic section presented by Snyder et al. (1996) to the east of Timor.

Crustal Shortening Estimates

The two balanced cross sections presented here provide minimum estimates for upper-crustal shortening during Banda–Australia collision. The eastern section has an original undeformed length of the Australian margin of 374 km, and the Banda Terrane has an undeformed length of 111 km, for a total undeformed length of the section of 485 km. The current deformed length of the eastern section is 159 km. This yields a minimum shortening estimate of 326 km, or 67%, in the eastern section. The western section has an original undeformed length of the Australian margin of 394 km, and the Banda Terrane has an undeformed length of 133 km. The total undeformed length of the orogen for the western section is therefore 527 km, while the current deformed length is 165 km. This yields a minimum shortening estimate of 362 km, or 69%, in the western section.

There are several important ways that these cross sections represent minimum shortening estimates. Several hanging-wall cutoffs have passed through the erosion surface, allowing for the possibility of some undocumented slip. However, the ubiquitous presence of Banda Terrane rocks above eroded hanging-wall cutoffs of the Gondwana Sequence duplex limits undocumented slip to a few kilometers. A larger potential source of undocumented shortening in our cross sections is within the Aileu slate and high-grade belts because (1) the difficulty constraining stratigraphic repetition has led us to use thrust sheets of maximum thickness, and (2) internal folding indicates significant ductile shortening in the Aileu high-grade belt (Berry and Grady, 1981; Prasetyadi and Harris 1996).

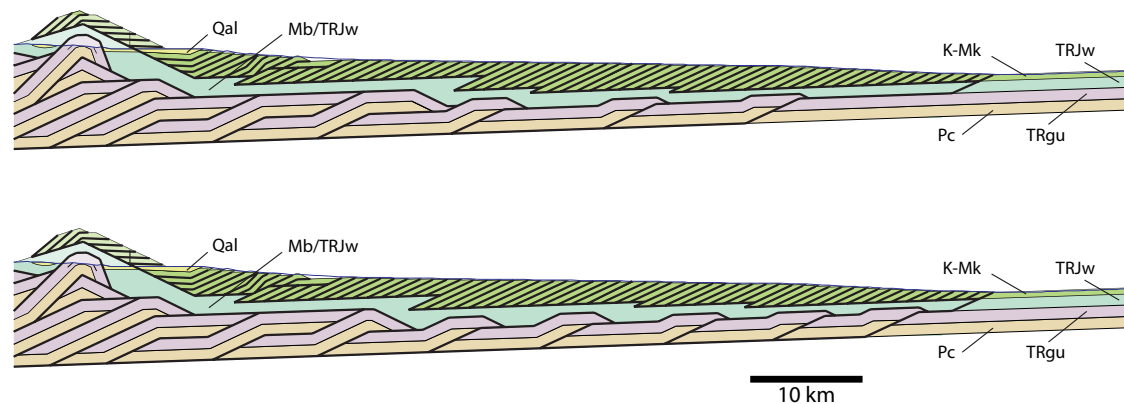


Figure 10. A possible alternative geometry of the offshore portion of the western cross section. Geometry from deformed section of Figure 9 below and alternative geometry above. Both geometries have the same shortening amount and restored margin length. No vertical exaggeration. Bold lines indicate faults; thin lines indicate stratigraphic contacts.

While these cross sections are broadly similar, a few notable differences exist between these two sections separated by only just over 40 km along strike. Shortening is 36 km larger in the western section, and the original length of the Australian paleomargin is 23 km longer in the western section. These differences may in part be due to undocumented shortening in our cross sections as detailed above. The map pattern, however, does suggest that more shortening has occurred along the western section than in the east because deeper structural levels are exposed on the south coast, and more Banda forearc has been underthrust exposing a wider Aileu Complex.

Some have suggested that the Aileu high-grade belt along the north coast is part of the Banda forearc (Kaneko et al., 2007) or was accreted to the Banda forearc prior to and separately from collision of Banda with the Australian margin (Audley-Charles, 2011; Ely et al., 2014) and thus does not contribute to Australian margin shortening estimates. If this is true, our cross sections would be drawn without the Aileu high-grade belt as part of the Australian margin, which would only remove 8 km of shortening in the eastern section and 9 km of shortening in the western section. Our shortening estimates are therefore not sensitive to interpretations of the affinity of the Aileu high-grade belt.

Quantifying Continental Subduction

The magnitude of continental subduction can be estimated using balanced cross section constraints and can be defined in one of two ways: (1) all material that has been incorporated into the orogenic wedge can be considered part of the upper plate, and all lower-crustal material that has passed under the deformation front (in our case south of Timor) is defined as subducted below the upper plate; or (2) lower-crustal material is defined as subducted not when it has passed the deformation front but only when it has passed beneath the undeformed backstop (in our case north of Timor). Because our study seeks primarily to shed light on the geodynamics of subducting buoyant continental crust below dense oceanic crust, and that buoyancy inversion takes place not when crust passes the deformation front but rather when crust passes below the island arc, we will use the second definition in our discussion.

The magnitude of Australian pre-Permian basement and mantle lithosphere that has been subducted beyond the undeformed backstop is calculated by taking the difference between the restored length of the Australian margin and the current distance from the Timor Trough to the Banda backstop in the Wetar Strait. For the eastern section, the restored length of the Australian margin is 374 km, while the current distance from the deformation front to the backstop is 159 km, yielding 215 km of continental subduction. For the western section, the restored length of the Australian margin is 394 km, while the current distance from the deformation front to the backstop is 165 km, yielding 229 km of continental subduction.

Similar to the effect on shortening magnitude, the magnitude of continental subduction is not highly sensitive to interpretations on the affinity

of the Aileu high-grade belt. Ascribing Banda or Sula Spur affinity to the Aileu high-grade belt would remove only 8 km of continental subduction from the eastern section and only 9 km of continental subduction from the western section.

Sequence of Deformation

The sequence of deformation suggested by our cross sections is illustrated in Figure 11. Muscovite $^{40}\text{Ar}/^{39}\text{Ar}$ closure at 7.1 ± 0.3 Ma in the Aileu high-grade belt (Tate et al., 2014) requires burial through generation of a structural high and subsequent exhumation within the Aileu high-grade belt at this time. We show this as the growth of an antiformal stack causing northward slumping. Thus overthrusting of the Banda forearc klippe must be before 7.1 ± 0.3 Ma. The period between 7.1 and 4.5 Ma was dominated by duplexing of the Aileu slate and Gondwana Sequence units. Tectonic erosion of Gondwana Sequence horses against the base of the Banda klippe requires some late thrusting of the Banda klippe after partial duplex construction, necessitating some amount of out-of-sequence deformation in the duplex. Additional out-of-sequence deformation is necessary to thrust Triassic units at Mount Cablac over the Lolotoi Complex. By 5.5 Ma, the steep sides of growing duplexes cause slumping of the Kolbano thrust belt away from the Banda klippe, creating the Viqueque basins (Tate et al., 2014). Backthrusting over part of the Banda forearc likely began ca. 4.5 Ma, corresponding to earliest zircon and apatite (U-Th)/He ages (Tate et al., 2014) and emergence of the island (indicated by lowland pollen within the Viqueque basins) (Nguyen et al., 2013). Along the western section, out-of-sequence thrusting along the Aileu-Maubisse thrust since the start of backthrusting over the Banda forearc is necessitated by the exhumation boundary observed at this thrust, as discussed in the Cross Section Constraints section (Tate et al., 2014). We propose that deformation of the Gondwana Sequence duplex shifted some of the deformation foreland of the Viqueque basin from 4.5 to 2.0 Ma in response to wedge-top sedimentation in the Viqueque basin. This foreland propagation of fold-thrust belt deformation in response to wedge-top sedimentation is consistent with geodynamic models (Fillon et al., 2013) and with young, 2.0 Ma to present cooling ages along the southernmost exposed structure along the western section. In addition, duplexing of underthrust Banda forearc below the Aileu Complex produces zircon (U-Th)/He ages younger than 2.0 Ma (Tate et al., 2014), and motion of the central Gondwana Sequence duplex over the foreland ramp to produce young (ca. 2 Ma) apatite (U-Th)/He ages (Tate et al., 2014).

The sequential reconstruction in Figure 11 provides constraints for variable shortening rates at Timor through time. Forty-six kilometers of shortening associated with Banda forearc overthrusting are documented before 7.1 ± 0.3 Ma, with an additional 8 km of shortening at ca. 7.1 Ma associated with Aileu high-grade belt deformation. Shortening of 147 km is documented between 7.1 and 4.5 Ma—a shortening rate of 57 km/m.y. Shortening of 55 km

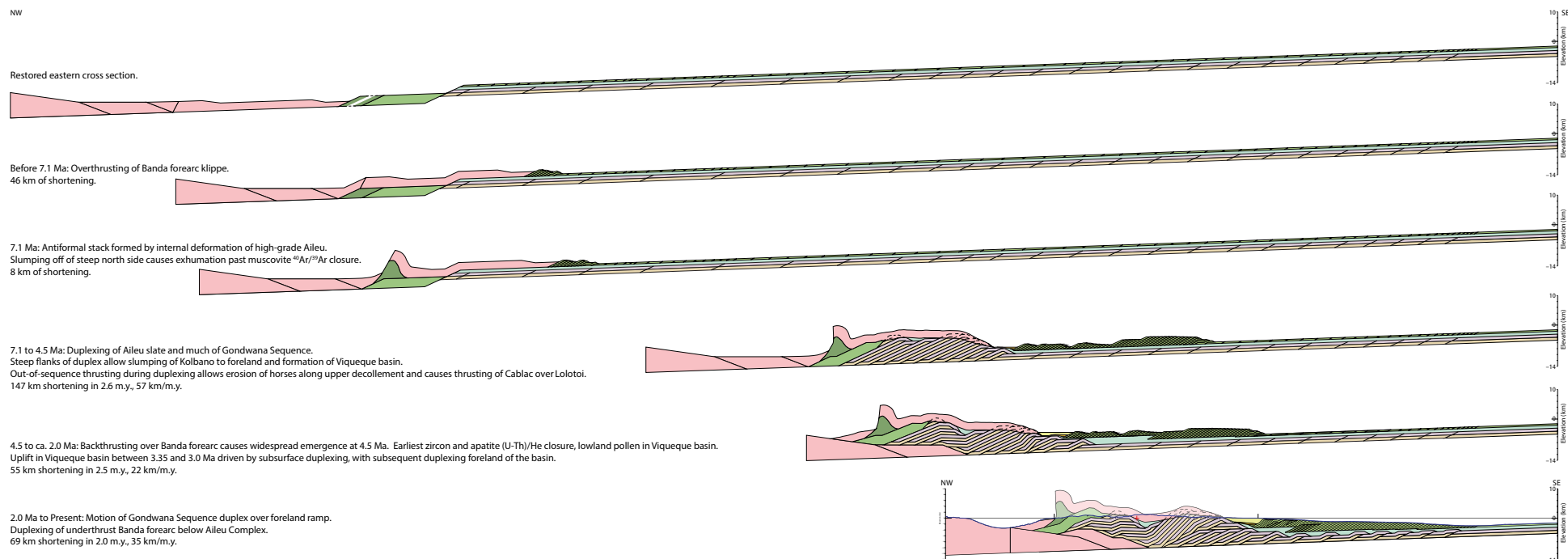


Figure 11. Sequential restoration of eastern cross section. No vertical exaggeration. From top: Restored eastern cross section. **Before 7.1 Ma:** Overthrusting of Banda forearc klippe; 46 km of shortening. **7.1 Ma:** Antiformal stack formed by internal deformation of high-grade Aileu; slumping off of steep north side causes exhumation past muscovite $^{40}\text{Ar}/^{39}\text{Ar}$ closure; 8 km of shortening. **7.1–4.5 Ma:** Duplexing of Aileu slate and much of Gondwana Sequence; steep flanks of duplex allow slumping of Kolbano to foreland and formation of Viqueque basin; out-of-sequence thrusting during duplexing allows erosion of horses along upper décollement and causes thrusting of Cablac over Lolotoi; 147 km shortening in 2.6 m.y., 57 km/m.y. **4.5 to ca. 2.0 Ma:** Backthrusting over Banda forearc causes widespread emergence at 4.5 Ma; earliest zircon and apatite (U-Th)/He closure, lowland pollen in Viqueque basin; uplift in Viqueque basin between 3.35 and 3.0 Ma driven by subsurface duplexing, with subsequent duplexing foreland of the basin; 55 km shortening in 2.5 m.y., 22 km/m.y. **2.0 Ma–present:** Motion of Gondwana Sequence duplex over foreland ramp; duplexing of underthrust Banda forearc below Aileu Complex; 69 km shortening in 2.0 m.y., 35 km/m.y.

is documented between 4.5 and ca. 2.0 Ma—a shortening rate of 22 km/m.y. Sixty-nine kilometers of shortening are documented from 2.0 Ma to the present—a shortening rate of 35 km/m.y. Although this suggests a change in shortening rate at 2.0 Ma, such a change is not rigorously constrained, because more foreland shortening of the Gondwana and Kolbano Sequences than is drawn here may have occurred prior to 2.0 Ma when out-of-sequence motion on the main southern ramp began. However, average shortening rates are distinctly faster prior to 4.5 Ma than after 4.5 Ma. We note that this change in shortening rate is coincident with the timing of emergence of Timor Island at 4.45 Ma (Nguyen et al., 2013). Additionally, subduction clogging and redistribution of shortening to the backarc may have influenced this decrease in shortening rate at Timor. We note also that shortening rates since 4.5 Ma are close to the modern GPS convergence rate of 22 mm/yr between Timor and Australia (Nugroho et al., 2009).

DISCUSSION

Timing of Initial Collision

These results constrain the timing of initial collision between the Banda forearc and the Australian margin. The maximum shortening rate is the plate convergence rate, ~ 70 km/m.y. (Nugroho et al., 2009; Spakman and Hall, 2010; Seton et al., 2012), which, combined with our shortening estimates, can help constrain the timing of deformation that occurred prior to available thermochronology dates. If the Aileu high-grade belt was part of the Australian margin during orogenesis at Timor, 46 km of shortening before 7.1 Ma implies initial collision of the Banda forearc with the Australian margin by at least 7.8 Ma. If instead the Aileu high-grade belt collided with the Banda forearc prior to and separately from collision at Timor, our sequential reconstruction would still

imply at least 193 km of shortening before 4.5 Ma, which would require initial collision by at least 7.3 Ma. We conclude, therefore, that initial collision of the Banda forearc and the Australian margin could not have been any more recent than 7.3 Ma. Because our shortening estimates indicate that initial collision must predate the 7.1 ± 0.3 Ma cooling of the Aileu high-grade belt, we also conclude that the 7.1 ± 0.3 Ma muscovite $^{40}\text{Ar}/^{39}\text{Ar}$ age (Tate et al., 2014) is associated with orogeny during collision of the Banda forearc and the Australian margin.

Comparison of Shortening to Plate Convergence and Absolute Plate Motions

Shortening estimates presented here are in good agreement with the rates of plate convergence predicted from plate reconstruction models and GPS observations. Australia is moving NNE relative to the oceanic Sunda-Banda lithosphere at a rate of ~ 7 cm/yr, according to relative plate reconstructions (Seton et al., 2012), absolute plate motion models (Spakman and Hall, 2010), and GPS observations (Nugroho et al., 2009). The relative plate motion vector of Australia versus the Sunda-Banda lithosphere as well as versus the mantle, however, is oblique to the Timor Trough and the structural trend of the Timor orogen. Trough-parallel motions may be accommodated through extrusion along proposed oblique normal faults on Timor (Duffy et al., 2013) or within or behind the Banda arc. The trough-perpendicular convergence rate (parallel to the trend of our cross sections) is ~ 53 mm/yr according to GPS vectors from Nugroho et al. (2009). This rate suggests ~ 360 – 392 km of trough-perpendicular convergence since 7.1 ± 0.3 Ma, the age of Aileu high-grade belt cooling through muscovite $^{40}\text{Ar}/^{39}\text{Ar}$ closure (Tate et al., 2014). (We compare plate convergence and shortening since 7.1 ± 0.3 Ma because the duration of earlier shortening in our reconstruction can only be constrained by the plate rate, as discussed above.) Our shortening estimates since 7.1 Ma are 270–303 km, which are the total shortening amounts minus Banda klippe overthrusting that in our cross sections must have occurred before Aileu exhumation at 7.1 Ma. If instead the Aileu high-grade belt collided with the Banda forearc separately from forearc collision with the Australian margin, our results indicate total shortening of 318–353 km since at least 7.3 Ma, whereas there has been 387 km of trough-perpendicular convergence since 7.3 Ma.

These shortening estimates from our cross sections are less than the trough-perpendicular convergence estimated from plate motions. The discrepancy between cross-section shortening and trough-perpendicular plate convergence can be accounted for by some combination of (1) missing shortening in our minimum shortening cross sections as discussed above, (2) overriding plate shortening north of Timor that is unaccounted for in our cross sections, and (3) wholesale subduction without underplating of upper-crustal material or underplating beyond the backstop. Silver et al. (1983) suggest 30–60 km of shortening along the well-developed Flores Thrust using seismic interpretation, sediment volumes within the accretionary wedge, and the displacement of the trend of the volcanic arc. North of Wetar (which is closer to the trend of

our cross sections), McCaffrey and Nabelek (1986) use the gravity signal of the small accretionary wedge to argue for less than 10 km of shortening specifically along the Wetar Thrust; although McCaffrey (1988) also suggests 50 km of total backarc shortening north of Wetar to accommodate the observed offset in the trend of the volcanic island chain between Wetar and Alor. Much of the shortening within the Wetar Strait between the Banda arc and Timor is already accounted for in our cross sections by backthrusting on the north side of Timor, although some additional shortening may have occurred along thrusts on the south side of the Banda arc (Snyder et al., 1996). North of Timor, 10–60 km of additional shortening increase total shortening estimates since 7.1 Ma to 280–363 km, a range that overlaps the 360–392 km of convergence estimated from plate motion. Moreover, there is a possibility that some additional Australian margin upper-crustal strata bypassed the thrust wedge at Timor and thus would not be included in our shortening estimates. Elburg et al. (2004) interpreted the chemical signal of contamination within Banda arc volcanics as the result of mixing between lower-continental crust and sedimentary rocks derived from the Australian upper crust. If these subducted sedimentary rocks were Permian or younger, that would indicate additional shortening not accounted for in our section.

Comparison to Other Arc-Continent Accretion Orogens

The orogen at Timor displays significantly more shortening and subduction of continental material than other prominent examples of arc-continent collision and continental underthrusting below oceanic crust (ophiolite emplacement). The Taiwan orogen is due to active collision between the Luzon volcanic arc and the Eurasian continental margin, with collision beginning in the late Miocene (latest arc volcanism provides a minimum age at 6 Ma) in the north and progressing to the south along this oblique margin over time (Huang et al., 2006). Suppe (1980) documents 160–200 km of shortening within the thin-skinned foreland fold-thrust belt of northern Taiwan. Although this would predict 126–202 km less shortening in Taiwan than we find in Timor, this estimate of 160–200 km of shortening in Taiwan does not include shortening within the slate belt or shortening due to overthrusting of the volcanic arc. Papua New Guinea is another example of arc-continent accretion, although accretion occurred from ca. 12 to 4 Ma and is no longer active (Hill and Raza, 1999). Hill (1991) documents only 43–60 km of shortening within the Papua New Guinea orogen, which is significantly less than shortening on Timor because deformation is dominated by inversion of extensional faults of the Australian margin. The thick-skinned structural style in Papua New Guinea is clearly visible in the surface geology, because granitic and metamorphic basement is exposed at the surface in the hanging wall of inverted normal faults (Hill, 1991). In Timor, however, the surface expression reveals the repetition of units in a thin-skinned structural style (the duplexing of Gondwana Sequence units), leading to significantly greater shortening. Ophiolite emplacement such as that over Arabia in Oman during the Late Cretaceous (Searle and Cox, 1999)

is not associated with the development of major fold-thrust belts such as in Timor but still exemplifies ~180 km of underthrusting of the continental margin below the overriding oceanic plate (McQuarrie and van Hinsbergen, 2013).

Magnitude of Continental Subduction

The balanced cross sections presented here suggest that 215–229 km of Australian continental crust have subducted beneath the Banda arc at Timor (Fig. 12). Continental subduction was long thought to be impossible because of buoyancy forces (McKenzie, 1969; Dewey and Bird, 1970). Subsequent models argued that continental subduction could be favored with removal of the top 10–20 km of the subducting continental lithosphere (Cloos, 1993; Capitanio et al., 2010). Our data, however, show significant continental subduction at Timor with only the top 3–4 km of upper stratigraphy removed and underplated to the overriding plate. Our magnitude of continental subduction is consistent with minimum depths of continental subduction of 100–120 km observed in UHP terranes (Chopin, 1984; Smith, 1984; Sobolev and Shatsky, 1990; Hermann and Rubatto, 2014), if those UHP terranes were subducted at an angle of ~30°. Early models of slab breakoff during continental collision suggest continental subduction to depths of 50–120 km or downdip lengths of 150–350 km, with subduction of continental crust to greater depths for convergence rates comparable to those at Timor (Davies and von Blanckenburg, 1995). More recent models suggest continental subduction of both upper and lower continental crust to depths of 125 km (Baumann et al., 2010), 200 km (van Hunen and Allen, 2011), or 300 km for oceanic crust of comparable age to that subducted at Timor (Duretz et al., 2011). Our subducted length of 215–229 km of continental crust is therefore consistent with numerical modeling for appropriately fast subduction rates and old subducted oceanic crust.

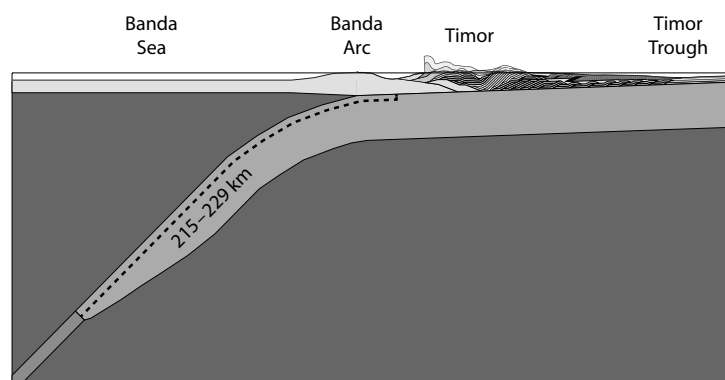


Figure 12. Schematic of 215–229 km of continental subduction. Magnitude of continental subduction is required to balance the length of restored Australian strata. Subducted Australian margin includes some length of transitional crust.

It is also possible that a significant portion of the subducted Australian margin was composed of transitional, thinned continental crust instead of continental crust of full thickness. Some portion of the Australian margin was likely composed of thinned continental crust formed during Jurassic rifting. Gondwana Sequence units, deposited prior to this rifting, were likely part of the stratigraphy of the transitional margin; thus the length of subducted Australian continental crust likely includes some length of transitional crust. The presence of occasional gabbro bodies within the Aileu high-grade belt along the north coast supports the possibility that these units derive from close to the ocean-continent transition. Transitional crust can greatly vary in strength and composition between the end members of continental and oceanic crust (Davies and von Blanckenburg, 1995), and a large portion of a transitional margin can even be negatively buoyant (Cloos, 1993; Cloos et al., 2005).

This documentation of continental subduction may allow a mechanism for recycling continental lithosphere into the mantle. Some models suggest that subducted continental material is exhumed to the base of the overriding plate following slab breakoff (Duretz et al., 2011), but some calculations suggest the possibility that transitional continental crust or continental crust effectively coupled to mantle lithosphere could remain negatively buoyant (Cloos, 1993; Cloos et al., 2005). Continental material fully subducted and recycled into the mantle may therefore have impacted the history of incompatible elements, heat-producing elements, and noble gases within the mantle.

CONCLUSIONS

New structural mapping and balanced cross sections in Timor-Leste have provided new insight into the process of arc-continent accretion. Mapping reveals that a 2 km succession of Australian strata has duplexed below overthrust Banda arc units to form the majority of the orogenic wedge. This observation necessitates large shortening amounts at Timor of 326–362 km. While many authors have assumed that continental subduction during arc-continent accretion is generally short lived (McKenzie, 1969; Dewey and Bird, 1970), we show that 215–229 km of Australian continental crust have subducted during arc-continent collision in Timor. This magnitude of continental subduction also has significant implications for the history of continental crust because it allows the possibility for substantial recycling of continental lithosphere at subduction zones.

ACKNOWLEDGMENTS

We thank the Office of the Secretary of State for Natural Resources in Timor-Leste for their assistance in completing fieldwork, particularly Norberta Soares da Costa, Jhony da Costa Soares, and Jhony Reis. Thanks are also due to Timorese geologists Lamberto Fernandes, Mario Amaral, Domingos Guterres, Octaviana de Jesus, and Romi Martin for their assistance in the field. This work was supported by National Science Foundation grant 0948449. D.J.J.v.H. was supported by European Research Council Starting Grant 306810 (Subduction Initiation reconstructed from Neothethyan Kinematics [SINK]) and acknowledges a Netherlands Organization for Scientific Research (NWO) VIDI grant number 864.11.004. R.R.B. acknowledges financial support from the Molengraaff Foundation. We appreciate very helpful reviews from Alex Webb, Tim Charlton, and Jeff Lee.

REFERENCES CITED

- Abbott, M.J., and Chamalaun, F.H., 1981, Geochronology of some Banda arc volcanics, in Barber, A.J., and Wiryosujono, S., eds., *The Geology and Tectonics of Eastern Indonesia*, volume 2: Bandung, Indonesia, Geological Research and Development Centre Special Publication, p. 253–268.
- Aben, F.M., Dekkers, M.J., Bakker, R., Van Hinsbergen, D.J.J., Zachariasse, J., Tate, G.W., McQuarrie, N., Harris, R., and Duffy, B., 2014, Untangling inconsistent magnetic polarity records through an integrated rock magnetic analysis: A case study on Neogene sections in East Timor: *Geochemistry Geophysics Geosystems*, v. 15, p. 2531–2554, doi:10.1002/2014GC005294.
- Agard, P., Omrani, J., Jolivet, L., Whitechurch, H., Vrielynck, B., Spakman, W., Monie, P., Meyer, B., and Wortel, R., 2011, Zagros orogeny: A subduction-dominated process: *Geological Magazine*, v. 148, no. 5–6, p. 692–725, doi:10.1017/S001675681100046X.
- Allmendinger, R.W., Cardozo, N.C., and Fisher, D., 2013, *Structural Geology Algorithms, Vectors, and Tensors*: Cambridge, England, Cambridge University Press, 289 p.
- Audley-Charles, M.G., 1965, Permian palaeogeography of the northern Australia-Timor region: *Palaeogeography, Palaeoclimatology, Palaeoecology*, v. 1, p. 297–305, doi:10.1016/0031-0182(65)90020-9.
- Audley-Charles, M.G., 1968, *The Geology of Portuguese Timor*: Geological Society of London Memoir 4, p. 4–84, doi:10.1144/GSL.MEM.1968.004.01.02.
- Audley-Charles, M.G., 1986, Rates of Neogene and Quaternary tectonic movement in the South Banda arc based on micropalaeontology: *Journal of the Geological Society of London*, v. 143, p. 161–175, doi:10.1144/gsjgs.143.1.0161.
- Audley-Charles, M.G., 2011, Tectonic post-collision processes in Timor, in Hall, R., and Cottam, M.A., eds., *The SE Asian Gateway: History and Tectonics of the Australia-Asia Collision*: Geological Society of London Special Publication 355, p. 241–266.
- Baumann, C., Gerya, T.V., and Connolly, J.A.D., 2010, Numerical modelling of spontaneous slab breakoff dynamics during continental collision, in Spalla, M.I., Mariotta, A.M., and Gosso, G., eds., *Advances in Interpretation of Geological Processes: Refinement of Multi-Scale Data and Integration in Numerical Modelling*: Geological Society, London, Special Publication 322, p. 99–114.
- Berry, R.F., 1981, Petrology of the Hili-Manu Lherzolite, East Timor: *Journal of the Geological Society of Australia*, v. 28, no. 3–4, p. 453–469, doi:10.1080/00167618108729181.
- Berry, R.F., and Grady, A.E., 1981, Deformation and Metamorphism of the Aileu Formation, North Coast, East Timor and Its Tectonic Significance: *Journal of Structural Geology*, v. 3, no. 2, p. 143–167, doi:10.1016/0191-8141(81)90011-0.
- Berry, R.F., and McDougall, I., 1986, Interpretation of $^{40}\text{Ar}/^{39}\text{Ar}$ and K/Ar dating evidence from the Aileu Formation, East-Timor, Indonesia: *Chemical Geology*, v. 59, no. 1, p. 43–58, doi:10.1016/0168-9622(86)90056-4.
- Bird, P.R., and Cook, S.E., 1991, Permo-Triassic successions of the Kekeno area, West Timor: Implications for palaeogeography and basin evolution: *Journal of Southeast Asian Earth Sciences*, v. 6, p. 359–371, doi:10.1016/0743-9547(91)90081-8.
- Capitanio, F.A., Morra, G., Goes, S., Weinberg, R.F., and Moresi, L., 2010, India-Asia convergence driven by the subduction of the Greater Indian continent: *Nature Geoscience*, v. 3, no. 2, p. 136–139, doi:10.1038/ngeo725.
- Cardozo, N., and Allmendinger, R.W., 2013, Spherical projections with OSXSTereonet: *Computers & Geosciences*, v. 51, p. 193–205, doi:10.1016/j.cageo.2012.07.021.
- Carter, D.J., Audley-Charles, M.G., and Barber, A.J., 1976, Stratigraphical analysis of island arc-continental margin collision in eastern Indonesia: *Journal of the Geological Society, London*, v. 132, no. 2, p. 179–198, doi:10.1144/gsjgs.132.2.0179.
- Charlton, T.R., 2002, The structural setting and tectonic significance of the Lolotoi, Laclubar, and Aileu metamorphic massifs, East Timor: *Journal of Asian Earth Sciences*, v. 20, no. 7, p. 851–865, doi:10.1016/S1367-9120(01)00075-X.
- Charlton, T.R., Barber, A.J., and Barkham, S.T., 1991, The structural evolution of the Timor collision complex, eastern Indonesia: *Journal of Structural Geology*, v. 13, no. 5, p. 489–500, doi:10.1016/0191-8141(91)90039-L.
- Charlton, T.R., and 13 others, 2002, The Permian of Timor: Stratigraphy, palaeontology and palaeogeography: *Journal of Asian Earth Sciences*, v. 20, no. 6, p. 719–774, doi:10.1016/S1367-9120(02)00018-4.
- Charlton, T.R., Barber, A.J., McGowan, A.J., Nicoll, R.S., Roniewicz, E., Cook, S.E., Barkham, S.T., and Bird, P.R., 2009, The Triassic of Timor: Lithostratigraphy, chronostratigraphy and palaeogeography: *Journal of Asian Earth Sciences*, v. 36, no. 4–5, p. 341–363, doi:10.1016/j.jseas.2009.06.004.
- Chen, P.F., Huang, B.S., and Liang, W.T., 2004, Evidence of a slab of subducted lithosphere beneath central Taiwan from seismic waveforms and travel times: *Earth and Planetary Science Letters*, v. 229, no. 1–2, p. 61–71, doi:10.1016/j.epsl.2004.10.031.
- Chopin, C., 1984, Coesite and pure pyrope in high-grade blueschists of the Western Alps: A first record and some consequences: *Contributions to Mineralogy and Petrology*, v. 86, no. 2, p. 107–118, doi:10.1007/BF00381838.
- Cloos, M., 1993, Lithospheric buoyancy and collisional orogenesis: Subduction of oceanic plateaus, continental margins, island arcs, spreading ridges, and seamounts: *Geological Society of America Bulletin*, v. 105, no. 6, p. 715–737, doi:10.1130/0016-7606(1993)105<0715:LBACOS>2.3.CO;2.
- Cloos, M., Sapiie, B., van Ufford, A.Q., Weiland, R.J., Warren, P.Q., and McMahon, T.P., 2005, Collisional delamination in New Guinea: The geotectonics of subducting slab breakoff: *Geological Society of America Special Paper* 400, 51 p.
- Cox, N.L., 2009, Variable uplift from Quaternary folding along the northern coast of East Timor, based on U-series age determinations of coral terraces: Salt Lake City, Utah, Department of Geological Sciences, Brigham Young University, 151 p.
- Davies, J.H., and von Blanckenburg, F., 1995, Slab Breakoff: A model of lithosphere detachment and its test in the magmatism and deformation of collisional orogens: *Earth and Planetary Science Letters*, v. 129, no. 1–4, p. 85–102, doi:10.1016/0012-821X(94)00237-S.
- Davydov, V.I., Haig, D.W., and McCartain, E., 2013, A latest Carboniferous warming spike recorded by a fusulinid-rich bioherm in Timor Leste: Implications for East Gondwana deglaciation: *Palaeogeography Palaeoclimatology Palaeoecology*, v. 376, p. 22–38, doi:10.1016/j.palaeo.2013.01.022.
- Davydov, V.I., Haig, D.W., and McCartain, E., 2014, Latest Carboniferous (late Gzhelian) fusulinids from Timor Leste and their paleobiogeographic affinities: *Journal of Paleontology*, v. 88, no. 3, p. 588–605, doi:10.1666/13-007.
- Dewey, J.F., and Bird, J.M., 1970, Mountain belts and new global tectonics: *Journal of Geophysical Research*, v. 75, no. 14, p. 2625–2647, doi:10.1029/JB075i014p02625.
- Dickinson, W.R., and Lawton, T.F., 2001, Carboniferous to Cretaceous assembly and fragmentation of Mexico: *Geological Society of America Bulletin*, v. 113, no. 9, p. 1142–1160, doi:10.1130/0016-7606(2001)113<1142:CTCAAF>2.0.CO;2.
- Duffy, B., Quigley, M., Harris, R., and Ring, U., 2013, Arc-parallel extrusion of the Timor sector of the Banda arc-continent collision: *Tectonics*, v. 32, p. 641–660, doi:10.1002/tect.20048.
- Duret, T., Gerya, T.V., and May, D.A., 2011, Numerical modelling of spontaneous slab breakoff and subsequent topographic response: *Tectonophysics*, v. 502, no. 1–2, p. 244–256, doi:10.1016/j.tecto.2010.05.024.
- Elburg, M.A., van Bergen, M.J., and Foden, J.D., 2004, Subducted upper and lower continental crust contributes to magmatism in the collision sector of the Sunda-Banda arc, Indonesia: *Geology*, v. 32, no. 1, p. 41–44, doi:10.1130/G19941.1.
- Ely, K.S., and Sandiford, M., 2010, Seismic response to slab rupture and variation in lithospheric structure beneath the Savu Sea, Indonesia: *Tectonophysics*, v. 483, no. 1–2, p. 112–124, doi:10.1016/j.tecto.2009.08.027.
- Ely, K.S., Sandiford, M., Hawke, M.L., Phillips, D., Quigley, M., and dos Reis, J.E., 2011, Evolution of Atauro Island: Temporal constraints on subduction processes beneath the Wetar zone, Banda arc: *Journal of Asian Earth Sciences*, v. 41, no. 6, p. 477–493, doi:10.1016/j.jseas.2011.01.019.
- Ely, K.S., Sandiford, M., Phillips, D., and Boger, S.D., 2014, Detrital zircon U-Pb and $^{40}\text{Ar}/^{39}\text{Ar}$ hornblende ages from the Aileu Complex, Timor-Leste: Provenance and metamorphic cooling history: *Journal of the Geological Society of London*, v. 171, no. 2, p. 299–309, doi:10.1144/jgs2012-065.
- Falloon, T.J., Berry, R.F., Robinson, P., and Stolz, A.J., 2006, Whole-rock geochemistry of the Hili Manu peridotite, East Timor: Implications for the origin of Timor ophiolites: *Australian Journal of Earth Sciences*, v. 53, no. 4, p. 637–649, doi:10.1080/08120090600686793.
- Fillon, C., Huisman, R.S., and van der Beek, P., 2013, Syntectonic sedimentation effects on the growth of fold-and-thrust belts: *Geology*, v. 41, no. 1, p. 83–86, doi:10.1130/G33531.1.
- Grady, A.E., and Berry, R.F., 1977, Some Palaeozoic–Mesozoic stratigraphic-structural relationships in East Timor and their significance in the tectonics of Timor: *Journal of the Geological Society of Australia*, v. 24, no. 4, p. 203–214, doi:10.1080/00167617708728981.
- Haig, D.W., and McCartain, E., 2007, Carbonate pelagites in the post-Gondwana succession (Cretaceous–Neogene) of East Timor: *Australian Journal of Earth Sciences*, v. 54, no. 6, p. 875–897, doi:10.1080/08120090701392739.

- Haig, D.W., and McCartain, E., 2010, Triassic organic-cemented siliceous agglutinated foraminifera from Timor Leste: Conservative Development in Shallow-Marine Environments: *Journal of Foraminiferal Research*, v. 40, no. 4, p. 366–392, doi:10.2113/gsfjr.40.4.366.
- Haig, D.W., McCartain, E., Barber, L., and Backhouse, J., 2007, Triassic–Lower Jurassic foraminiferal indices for Bahaman-type carbonate-bank limestones, Cablac Mountain, East Timor: *Journal of Foraminiferal Research*, v. 37, no. 3, p. 248–264, doi:10.2113/gsfjr.37.3.248.
- Hall, R., 2002, Cenozoic geological and plate tectonic evolution of SE Asia and the SW Pacific: Computer-based reconstructions, model and animations: *Journal of Asian Earth Sciences*, v. 20, no. 4, p. 353–431, doi:10.1016/S1367-9120(01)00069-4.
- Harris, R., 1991, Temporal distribution of strain in the active Banda orogen: A reconciliation of rival hypotheses: *Journal of Southeast Asian Earth Sciences*, v. 6, p. 373–386, doi:10.1016/0743-9547(91)90082-9.
- Harris, R., 2006, Rise and fall of the Eastern Great Indonesian arc recorded by the assembly, dispersion and accretion of the Banda Terrane, Timor: *Gondwana Research*, v. 10, no. 3–4, p. 207–231, doi:10.1016/j.gr.2006.05.010.
- Harris, R., 2011, The Nature of the Banda Arc-Continent Collision in the Timor Region, in Brown, D., and Ryan, P.D., eds., *Arc-Continent Collision: Berlin, Heidelberg, Springer*, p. 163–211.
- Harris, R., and Long, T., 2000, The Timor ophiolite, Indonesia: Model or myth? in Dilek, Y. et al., eds., *Ophiolites and Oceanic Crust: New Insights from Field Studies and the Ocean Drilling Program: Geological Society of America Special Paper 349*, p. 321–330.
- Harris, R., Sawyer, R.K., and Audley-Charles, M.G., 1998, Collisional mélange development: Geologic associations of active mélange-forming processes with exhumed mélange facies in the western Banda orogen, Indonesia: *Tectonics*, v. 17, no. 3, p. 458–479, doi:10.1029/97TC03083.
- Harris, R., Kaiser, J., Hurford, A., and Carter, A., 2000, Thermal history of Australian passive margin cover sequences accreted to Timor during Late Neogene arc-continent collision, Indonesia: *Journal of Asian Earth Sciences*, v. 18, no. 1, p. 47–69, doi:10.1016/S1367-9120(99)00036-X.
- Harris, R., Vorkink, M.W., Prasetyadi, C., Zobell, E., Roosmawati, N., and Aphorpe, M., 2009, Transition from subduction to arc-continent collision: Geologic and neotectonic evolution of Savu Island, Indonesia: *Geosphere*, v. 5, no. 3, p. 152–171, doi:10.1130/GES00209.1.
- Hermann, J., and Rubatto, D., 2014, Subduction of Continental Crust to Mantle Depth: Geochemistry of Ultrahigh-Pressure Rocks, in Holland H., and Turekian, K., eds., *Treatise on Geochemistry: Amsterdam, Netherlands, Elsevier*.
- Herrington, R.J., Scotney, P.M., Roberts, S., Boyce, A.J., and Harrison, D., 2011, Temporal association of arc-continent collision, progressive magma contamination in arc volcanism and formation of gold-rich massive sulphide deposits on Wetar Island (Banda arc): *Gondwana Research*, v. 19, no. 3, p. 583–593, doi:10.1016/j.gr.2010.10.011.
- Hill, K.C., 1991, Structure of the Papuan fold belt, Papua New Guinea: *American Association of Petroleum Geologists Bulletin*, v. 75, no. 5, p. 857–872.
- Hill, K.C., and Raza, A., 1999, Arc-continent collision in Papua Guinea: Constraints from fission track thermochronology: *Tectonics*, v. 18, no. 6, p. 950–966, doi:10.1029/1999TC900043.
- Huang, C.Y., Yuan, P.B., Lin, C.W., Wang, T.K., and Chang, C.P., 2000, Geodynamic processes of Taiwan arc-continent collision and comparison with analogs in Timor, Papua New Guinea, Urals and Corsica: *Tectonophysics*, v. 325, no. 1–2, p. 1–21, doi:10.1016/S0040-1951(00)00128-1.
- Huang, C.Y., Yuan, P.B., and Tsao, S.J., 2006, Temporal and spatial records of active arc-continent collision in Taiwan: A synthesis: *Geological Society of America Bulletin*, v. 118, no. 3–4, p. 274–288, doi:10.1130/B25527.1.
- Kaneko, Y., Maruyama, S., Kadarusman, A., Ota, T., Ishikawa, M., Tsujimori, T., Ishikawa, A., and Okamoto, K., 2007, On-going orogeny in the outer-arc of the Timor-Tanimbar region, eastern Indonesia: *Gondwana Research*, v. 11, no. 1–2, p. 218–233, doi:10.1016/j.gr.2006.04.013.
- Keep, M., and Haig, D.W., 2010, Deformation and exhumation in Timor: Distinct stages of a young orogeny: *Tectonophysics*, v. 483, no. 1–2, p. 93–111, doi:10.1016/j.tecto.2009.11.018.
- Long, S., McQuarrie, N., Tobgay, T., and Grujic, D., 2011, Geometry and crustal shortening of the Himalayan fold-thrust belt, eastern and central Bhutan: *Geological Society of America Bulletin*, v. 123, no. 7–8, p. 1427–1447.
- McCaffrey, R., 1988, Active tectonics of the Eastern Sunda and Banda arcs: *Journal of Geophysical Research—Solid Earth*, v. 93, B12, p. 15,163–15,182, doi:10.1029/JB093iB12p15163.
- McCaffrey, R., and Nabelek, J., 1986, Seismological evidence for shallow thrusting north of the Timor trough: *Geophysical Journal International*, v. 85, no. 2, p. 365–381, doi:10.1111/j.1365-246X.1986.tb04518.x.
- McCaffrey, R., Molnar, P., Roecker, S.W., and Joyodiwiroyo, Y.S., 1985, Microearthquake seismicity and fault plane solutions related to arc-continent collision in the eastern Sunda arc, Indonesia: *Journal of Geophysical Research*, v. 90, p. 4511–4528.
- McCartain, E., Backhouse, J., Haig, D., Balme, B., and Keep, M., 2006, Gondwana-related Late Permian palynoflora, foraminifers and lithofacies from the Wailuli Valley, Timor Leste: *Neues Jahrbuch für Geologie und Paläontologie-Abhandlungen*, v. 240, no. 1, p. 53–80.
- McKenzie, D.P., 1969, Speculations on the Consequences and Causes of Plate Motions: *Geophysical Journal International*, v. 18, no. 1, p. 1–32, doi:10.1111/j.1365-246X.1969.tb00259.x.
- McQuarrie, N., and van Hinsbergen, D.J.J., 2013, Retrodeforming the Arabia-Eurasia collision zone: Age of collision versus magnitude of continental subduction: *Geology*, v. 41, no. 3, p. 315–318, doi:10.1130/G33591.1.
- Mouthereau, F., Lacombe, O., and Verges, J., 2012, Building the Zagros collisional orogen: Timing, strain distribution and the dynamics of Arabia/Eurasia plate convergence: *Tectonophysics*, v. 532, p. 27–60, doi:10.1016/j.tecto.2012.01.022.
- Nguyen, N., Duffy, B., Shulmeister, J., and Quigley, M., 2013, Rapid Pliocene uplift of Timor: *Geology*, v. 41, p. 179–182.
- Nugroho, H., Harris, R., Lestariya, A.W., and Maruf, B., 2009, Plate boundary reorganization in the active Banda arc-continent collision: Insights from new GPS measurements: *Tectonophysics*, v. 479, no. 1–2, p. 52–65, doi:10.1016/j.tecto.2009.01.026.
- Orchard, M.J., 2010, Triassic conodonts and their role in stage boundary definition, in Lucas, S.G., ed., *The Triassic Timescale: Geological Society, London, Special Publications*, v. 334, no. 1, p. 139–161, doi:10.1144/SP334.7.
- Prasetyadi, C., and Harris, R., 1996, Structure and Tectonic Significance of the Aileu Formation East Timor, Indonesia: *Proceedings of the 25th Annual Convention of the Indonesian Association of Geologists*, p. 144–173.
- Richardson, A.N., and Blundell, D.J., 1996, Continental collision in the Banda arc: *Geological Society of London Special Publications*, v. 106, p. 47–60, doi:10.1144/GSL.SP.1996.106.01.05.
- Roosmawati, N., and Harris, R., 2009, Surface uplift history of the incipient Banda arc-continent collision: *Geology and synorogenic foraminifera of Rote and Savu Islands, Indonesia: Tectonophysics*, v. 479, no. 1–2, p. 95–110, doi:10.1016/j.tecto.2009.04.009.
- Rosidi, H.M.D., Tjokrosapetro, S., and Gafoer, S., 1979, *Geological Map of the Kupang-Atambua Quadrangles, Timor: Indonesia, Geological Research and Development Centre*.
- Sandiford, M., 2008, Seismic moment release during slab rupture beneath the Banda Sea: *Geophysical Journal International*, v. 174, no. 2, p. 659–671, doi:10.1111/j.1365-246X.2008.03838.x.
- Sani, K., Jacobson, M.I., and Sigit, R., 1995, The thin-skinned thrust structures of Timor: 24th Annual Convention Proceedings, Indonesian Petroleum Association, p. 277–293.
- Sawyer, R.K., Sani, K., and Brown, S., 1993, *The Stratigraphy and Sedimentology of West Timor, Indonesia: Jakarta, Proceedings of the Indonesian Petroleum Association*, p. 1–20.
- Searle, M., and Cox, J., 1999, Tectonic setting, origin, and obduction of the Oman ophiolite: *Geological Society of America Bulletin*, v. 111, no. 1, p. 104–122, doi:10.1130/0016-7606(1999)111<0104:TSAOO>2.3.CO;2.
- Şengör, A.M.C., Natalin, B.A., and Burtman, V.S., 1993, Evolution of the Altaid tectonic collage and Paleozoic crustal growth in Eurasia: *Nature*, v. 364, no. 6435, p. 299–307, doi:10.1038/364299a0.
- Seton, M., and 10 others, 2012, Global continental and ocean basin reconstructions since 200 Ma: *Earth-Science Reviews*, v. 113, no. 3–4, p. 212–270, doi:10.1016/j.earscirev.2012.03.002.
- Shulgin, A., Kopp, H., Mueller, C., Lueschen, E., Planert, L., Engels, M., Flueh, E.R., Krabbenhoft, A., and Djajadihardja, Y., 2009, Sunda-Banda arc transition: Incipient continent-island arc collision (northwest Australia): *Geophysical Research Letters*, v. 36, doi:10.1029/2009GL037533.
- Silver, E.A., Reed, D., McCaffrey, R., and Joyodiwiroyo, Y., 1983, Back arc thrusting in the eastern Sunda arc, Indonesia: A consequence of arc-continent collision: *Journal of Geophysical Research*, v. 88, no. 9, p. 7429–7448.
- Smith, D.C., 1984, Coesite in clinopyroxene in the Caledonides and its implications for geodynamics: *Nature*, v. 310, no. 5979, p. 641–644, doi:10.1038/310641a0.
- Smith, W.H.F., and Sandwell, D.T., 1997, Global sea floor topography from satellite altimetry and ship depth soundings: *Science*, v. 277, no. 5334, p. 1956–1962, doi:10.1126/science.277.5334.1956.
- Snyder, D.B., Prasetyo, H., Blundell, D.J., Pigram, C.J., Barber, A.J., Richardson, A., and Tjokrosapetro, S., 1996, A dual doubly vergent orogen in the Banda arc continent arc collision zone as observed on deep seismic reflection profiles: *Tectonics*, v. 15, no. 1, p. 34–53, doi:10.1029/95TC02352.
- Sobolev, N.V., and Shatsky, V.S., 1990, Diamond inclusions in garnets from metamorphic rocks: A new environment for diamond formation: *Nature*, v. 343, no. 6260, p. 742–746, doi:10.1038/343742a0.

- Spakman, W., and Hall, R., 2010, Surface deformation and slab-mantle interaction during Banda arc subduction rollback: *Nature Geoscience*, v. 3, no. 8, p. 562–566, doi:10.1038/ngeo917.
- Standley, C.E., and Harris, R., 2009, Tectonic evolution of forearc nappes of the active Banda arc-continent collision: Origin, age, metamorphic history and structure of the Lolotoi Complex, East Timor: *Tectonophysics*, v. 479, no. 1–2, p. 66–94, doi:10.1016/j.tecto.2009.01.034.
- Suppe, J., 1980, A retrodeformable cross section of northern Taiwan: *Proceedings of the Geological Society of China*, v. 23, p. 46–55.
- Suppe, J., 1983, Geometry and kinematics of fault-bend folding: *American Journal of Science*, v. 283, no. 7, p. 684–721, doi:10.2475/ajs.283.7.684.
- Tate, G.W., McQuarrie, N., van Hinsbergen, D.J.J., Bakker, R., Harris, R., Willett, S.D., Reiners, P.W., Fellin, M.G., Ganerod, M., and Zachariasse, J., 2014, Resolving spatial heterogeneities in exhumation and surface uplift in Timor-Leste: Constraints on deformation processes in young orogens: *Tectonics*, v. 33, no. 6, p. 1089–1112, doi:10.1002/2013TC003436.
- van Hinsbergen, D.J.J., Hafkenscheid, E., Spakman, W., Meulenkamp, J.E., and Wortel, R., 2005, Nappe stacking resulting from continental lithosphere below subduction of oceanic and Greece: *Geology*, v. 33, no. 4, p. 325–328.
- van Hinsbergen, D.J.J., Kaymakci, N., Spakman, W., and Torsvik, T.H., 2010, Reconciling the geological history of western Turkey with plate circuits and mantle tomography: *Earth and Planetary Science Letters*, v. 297, no. 3–4, p. 674–686, doi:10.1016/j.epsl.2010.07.024.
- van Hunen, J., and Allen, M.B., 2011, Continental collision and slab break-off: A comparison of 3-D numerical models with observations: *Earth and Planetary Science Letters*, v. 302, no. 1–2, p. 27–37, doi:10.1016/j.epsl.2010.11.035.
- Wilson, J.T., 1966, Did the Atlantic Close and Then Re-Open?: *Nature*, v. 211, no. 5050, p. 676–681, doi:10.1038/211676a0.
- Zobell, E.A., 2007, Origin and tectonic evolution of Gondwana Sequence units accreted to the Banda arc: A structural transect through central East Timor [M.S. thesis]: Provo, Utah, Brigham Young University, 75 p.